

ESIS

This is to certify that the

- dissertation entitled

SURFACE-MODIFIED IMOCOLITE: COUPLING REACTIONS AND Na-MONTMORILLONITE INTERCALATION **PRODUCTS** 

presented by

Leighta Maureen Johnson

has been accepted towards fulfillment of the requirements for

degree in Chemistry Ph.D.

MSU is an Affirmative Action/Equal Opportunity Institution

0-12771

# PLACE IN RETURN BOX to remove this checkout from your record. TO AVOID FINES return on or before date due.

DATE DUE	DATE DUE	DATE DUE
(512 2 5 - 2 5 (1 2 6 5 5		

MSU is An Affirmative Action/Equal Opportunity Institution choicedeseus.pm3-p.1

al.

# SURFACE-MODIFIED IMOGOLITE: COUPLING REACTIONS AND Na-MONTMORILLONITE INTERCALATION PRODUCTS

Ву

Leighta Maureen Johnson

#### A DISSERTATION

Submitted to
Michigan State University
in partial fulfillment of the requirements
for the degree of

DOCTOR OF PHILOSOPHY

Department of Chemistry

1991

#### ABSTRACT

# SURFACE-MODIFIED IMOGOLITE: COUPLING REACTIONS AND Na-MONTMORILLONITE INTERCALATION PRODUCTS

By

#### Leighta Maureen Johnson

The tubular aluminosilicate, imogolite, having a diameter of 23 Å, a length of 2000 to 3000 Å and an internal channel diameter of ≈8.7 Å was the material of interest in this study. Imogolite intercalates as a regular monolayer between the layers of Na-montmorillonite clay. The intercalated tubes align in van der Waals contact with one another and the clay layer. Therefore, the microporosity of this tubular silicate layered silicate, TSLS complex was restricted to the internal tube channels.

The focus of this work was concerted catalyst design. Modification of the external surfaces of imogolite was investigated as a possible route for enhancement of the microporosity of the TSLS complex. Surface modification was envisioned to promote lateral separation between the Na-montmorillonite intercalated surface-modified tubes. Removal of the surface-modifying agent by calcination might yield highly microporous products.

The internal and external surfaces of imogolite were silylated by allowing gamma-aminopropyltriethoxysilane (APS) to react with imogolite suspensions in acidic

solution. The hydrolytic lability of the APS-modified imogolite was examined by monitoring the depletion of siloxane polymer from the tubular surfaces by dialysis against water at ambient pH. Bimodal depletion behavior was observed for APS-modified imogolite. This behavior was attributed to differences in the hydrolytic lability for siloxane polymer bound at the internal SiOH surfaces and the external AlOH surfaces. Covalent bonding between APS and imogolite SiOH sites was detected in the <sup>1</sup>H decoupled <sup>29</sup>Si MAS NMR spectrum of the APS-modified material. Polymer hydrolysis prevented the formation of ordered APS-modified imogolite intercalated products.

Gamma-aminopropylphosphonic acid (APP) was found both to chemisorb to the external  $Al(H_2O)^+$  imagolite surface and to intercalate within the tube channel. Highly ordered washed products were obtained from APP-modified imagolite intercalated Na-montmorillonite at neutral pH. <sup>29</sup>Si and <sup>1</sup>H decoupled <sup>31</sup>P MAS NMR, FTIR, x-ray diffraction, elemental analysis and adsorption measurements were characterize the material. The products were identified as quadruple layer of close-packed imogolite tubes intercalated between the layers of Na-montmorillonite. Reactions of APP with Na-montmorillonite yielded ordered intersalate compounds of APP or APP/APP depending upon the reaction pH.

To my family and Phil

#### **ACKNOWLEDGMENTS**

I would like to thank Dr. T.J. Pinnavaia for his guidance and financial support throughout the course of this work. I truly respect his skill as a teacher. Now I can appreciate many of the things he taught me, although I didn't know I was learning them at the time. The outcome of the chemistry was unpredictable, but I could always rely on his special ability to provide an alternate point of view. I hope to continue to have the opportunity to exchange ideas in the future.

I am very grateful to Dr. Eick for his efforts as the second reader of this manuscript. I appreciate his commitment and cooperation under the time constraints involved.

I would also like to express my gratitude to my husband, for his efforts to allow me to concentrate more fully on my work.

I would like to thank Kermit Johnson and Dr. Yesinowski for their technical assistance and consultation.

I would also like to thank the members of the Pinnavaia group for their helpful discussion and support.

Finally, I would like to thank Ahmad Moini and Kirk Schmitt of Mobil Research and Development Corporation for

providing critical  $^{31}\text{P}$  NMR spectra when the equipment at MSU was being repaired.

### TABLE OF CONTENTS

			Page
LIST	OF I	TABLES	ix
LIST	OF F	FIGURES	x
		Introduction	
_	Α.	Historical Significance	1
	В.	Imogolite	
1	c.	Na-Montmorillonite	_ 5
	D.	Tubular Silicate Layered Silicate, TSLS	<u> </u>
	Ε.	Research Objectives	. 7
	F.	APS-modified Imogolite/Na-montmorillonite	10
(	G.	Phosphorus Acid Coupled Alumina Surfaces	_ 11
	н.	APP-modified Imogolite/Na-montmorillonite	13
	I.	List of References	15
Polym	er (	I Silylation of a Tubular Aluminosilicate Imogolite), by Reaction with Hydrolyzed gamma-pyltriethoxysilane (APS).	,
į	A.	Introduction	17
1	в.	Experimental	. 19
(	c.	Results	20
. 1	D.	Discussion	31
1	E.	List of References	36
and I	nter	II Hydrolytic Lability of Silylated Imogolicalation of the Silylated Tubular, Aluminosilicallonite.	
i	A.	Introduction	39
1	в.	Experimental	40

		Page
c.	Results	_ 44
D.	Discussion	_ 61
Ε.	List of References	_ 67
	Reaction of Gamma-aminopropylphosphonic olite and Na-montmorillonite.	acid
A.	Introduction	_ 69
в.	Experimental	71
c.	Results and Discussion	_ 73
D.	Conclusions	_ 103
E.	List of References	105

### LIST OF TABLES

<u>Table</u>	age
II.I. FTIR vibrational frequencies (cm <sup>-1</sup> ) for hydrolyzed APS and hydrolyzed APS-imogolite reaction products	28
III.I. <sup>29</sup> Si chemical shifts for silicon environments in pristine APS polymer, APS-modified Imogolite and APS-modified gamma-alumina	57
IV.I. Acid dissociation constants and <sup>31</sup> P chemical shifts for gamma-aminopropylphosphonic acid species in aqueous solution and isolated in the solid state	75
IV.II. Selected IR Frequencies (cm <sup>-1</sup> ) for solid APP recovered from solution at different pH values	76
IV.III. Selected IR Frequencies (cm <sup>-1</sup> ) (KBr pellet) for APP-modified systems	82
IV.IV. 1H decoupled 31P MAS NMR resonances observed for APP-modified systems	83
IV.V. Elemental Analysis results for the APP-coupled Na-montmorillonite and APP-coupled imogolie intercalated montmorillonite samples	92
IV.VI. Ratio of the areas obtained by deconvolution analysis of 29Si NMR resonances at -79 ppm (imogolite) and -93 ppm (Na-montmorillonite), and the corresponding imogolite:clay wt. ratios	100

## LIST OF FIGURES

<u>Page</u>
Figure I.1. Idealized structural representation of the cross section of the imogolite tube2
Figure I.2. Idealized structure of Na-montmorillonite. Silicon atoms occupy the tetrahedral positions in the oxygen framework, aluminum or magnesium atoms occupy the octahedral sites. M <sup>n+</sup> represents the interlayer Na cation.
Figure I.3. Schematic representation of TSLS 8
Figure II.1. Cross-sectional view of the tubular aluminosilicate imogolite (adapted from reference 22). The inner and outer tube diameters are - 8.2 Å and 23 Å, respectively. Tube lengths of the synthetic derivative used in the present work are typically from 250 to 350 nm. The empirical formula, as read from outer to inner atomic planes is (HO) <sub>3</sub> Al <sub>2</sub> O <sub>3</sub> Si(OH)
Figure II.2. FTIR spectra (KBr disks) of (A) APS polymer prepared by hydrolysis and drying in air; (B) APS polymer prepared by hydrolysis in acetic acid at pH 3.6 and air drying; and (C) synthetic imogolite22
Figure II.3. FTIR spectra (KBr disks) of silylated imogolite reaction products formed at formal APS: Al molar ratios of (A) 0.5: 1, (B) 1: 1, (C) 2: 1, (D) 2.5: 1.
Figure II.4. FTIR difference spectra for the region between 800 cm <sup>-1</sup> and 2000 cm <sup>-1</sup> obtained by digital subtraction of the imogolite spectrum in Figure II.2C from the spectra for the APS-imogolite reaction products in Figure II.3.
Figure II.5. <sup>29</sup> Si MAS NMR spectra: (A) the pure siloxane polymer obtained by hydrolysis in aqueous acetic acid at pH 3.6; (B) the pure siloxane polymer obtained by hydrolysis in water; (C) the acid-hydrolyzed APS-imogolite reaction product obtained at a formal APS: Al ratio of 0.5: 1.0.

Figure	Page
Figure III.1. FTIR absorbance spectra (KBr pellets) of the substrates (A) imagolite and (B) gamma-alumina.	47
Figure III.2. FTIR absorbance spectra (KBr pellets) of APS-modified imogolite samples isolated after dialys for the time intervals indicated.	is 49
Figure III.3. FTIR absorbance spectra (KBr pellets) of APS-modified gamma-alumina samples isolated after dialysis for the time intervals indicated	50
Figure III.4. Plot of log(wt. % APS) versus dialysis time for the hydrolyzed APS polymer, APS-modified imogolite and APS-modified gamma-alumina.	53
Figure III.5. <sup>1</sup> H decoupled <sup>29</sup> Si MAS NMR (79.459MHz) spectra of (A) 20 wt. % APS-modified imagolite and (B) 24 wt. % APS-modified gamma-alumina samples using a 3 us pulse width, a relaxation delay time of 20 s, and a sample spinning rate of 5 kHz.	: 55
Figure III.6. X-ray diffraction patterns of oriented films of (A) Na-montmorillonite, (B) 57 wt. % APS-modified Na-montmorillonite, (C) sample in (B) washed once with $H_2O$ , and (D) sample in (B) washed twice with $H_2O$ .	. 59
Figure III.7. X-ray diffraction patterns of oriented films of (A) 7 wt. % APS-modified imagolite suspension combined with a Na-montmorillonite suspension in a wt. ratio of 2.5:1 imagolite to clay, (B) sample in (A) washed once with water and (C) sample in (A) washed twice with water.	60
Figure III.8. Schematic representation of a cross sectional view of the imogolite structure. The tube walls are composed of five tiers of atoms. Reading from the inner to the outer wall, the tier compositions are HO, Si, O, Al, and OH, respectively. The diameter of the channel, 8.7 Å, is sufficiently large to accomodate APS as a silylating agent.	64
Figure IV.1 <sup>1</sup> H decoupled <sup>31</sup> P MAS NMR spectrum (161.903 MHz) of solid gamma-aminopropylphosphonic acid as received, obtained with a pulse width of 4.8 usec, a relaxation delay time of 60 seconds and a sample spinning rate of 4KHz.	. 80
Figure IV.2 X-ray diffraction patterns of (A) APPMONT (B) APPMONTA washed once with water and (C) APPMONTA washed twice with water.	' <b>A,</b> 87

<u>Figure</u> P	<u>age</u>
Figure IV.3 X-ray diffraction patterns of (A) APPMONTB (B) APPMONTB washed once with water and (C) APPMONTB washed twice with water.	, 89
Figure IV.4 FTIR difference spectra (KBr Pellets) of (A) APPMONTA and (B) APPMONTB.	90
Figure IV.5 X-ray diffraction patterns of (A) APPIIM55 and (B) APPIIM55 after heating at 130°C in air for 48 h.	
Figure IV.6 X-ray diffraction pattern of APPIIM75	97
Figure IV.7 <sup>1</sup> H decoupled <sup>31</sup> P MAS NMR spectrum (145.76 MHz) of APPIIM75, obtained with a 3 usec pulse width and a relaxation delay time of 62 sec. (Spectrum courtesy of Kirk Schmitt, Mobil Research and Development Corporation).	98

#### CHAPTER I

#### Introduction

#### A. HISTORICAL SIGNIFICANCE

A wide variety of applications are known to utilize surface chemistry of aluminas. effectiveness of aluminas as adsorbant materials has led to application of these oxides the in chromatographic separations processes. 1 The thermal stability and high surface area of aluminum oxides has prompted their use as catalysts and catalyst supports.<sup>2,3</sup> Surface modification of aluminas has improved their performance in each of these applications. 4-6 The work described here incorporates the use of coupling agents for surface modification, in order to develop superior microporous materials for catalysis applications.

#### B. IMOGOLITE

The external aluminum hydroxide surfaces of the tubular aluminosilicate, imogolite, were selected for surface modification in this study. Figure I.1 shows a schematic representation of a cross section of the imogolite tube. The tube diameter is  $\approx 23$  Å, and the internal cavity diameter is 8.7 Å. The length of the

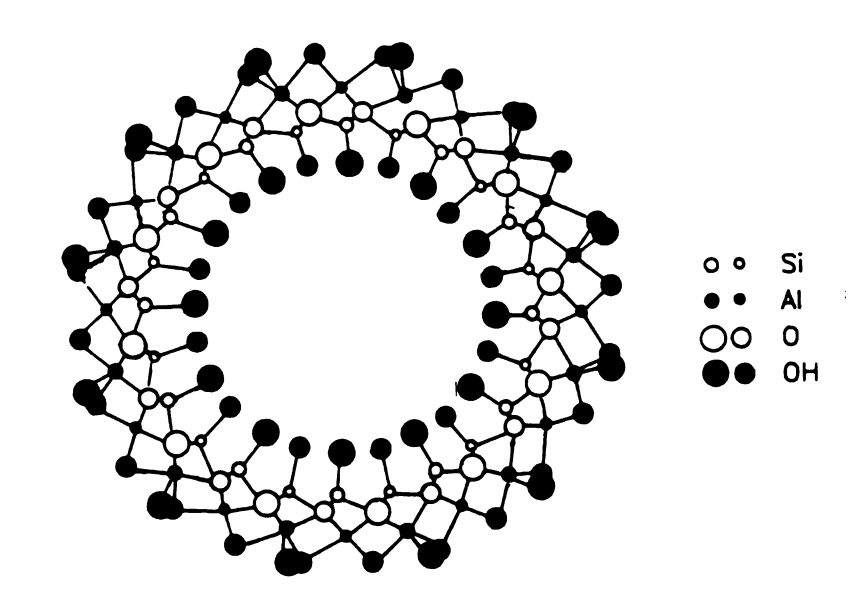


Figure I.3. Schematic representation of TSLS.

imogolite tubes, as synthesized by the method described by Farmer and Fraser<sup>8</sup>, was determined by electron microscopy. The tube lengths ranged between 2000 and 3000 Å. Imogolite has also been characterized by FTIR and <sup>29</sup>Si MAS NMR spectroscopy.<sup>9,10</sup>

Certain physical and structural properties of imogolite make it attractive as a potential catalyst material. Imogolite is a very high surface area material due to the internal cavity and small particle size. The hydroxylated nature of both the internal cavity and the external surfaces of the tube, give rise to water-clear aqueous imogolite suspensions under conditions of reduced pH and concentrations <0.4 wt. %. Particle aggregation is initiated at elevated concentration and pH, resulting in gelation of the imogolite sol particles. A more complete review of the imogolite literature has been presented in previous work. 11

The adsorption properties of imogolite has been studied by several different groups. Theng et al. 12 investigated the pH dependent adsorption of Na and Cl ions on natural imogolite. Natural imogolite was found to possess the highest positive surface charge at pH 4. Chloride adsorption occurs at Al-OH-Al sites on the external surfaces of the tubes, which become protonated at low pH. A chloride adsorption capacity of 35 meq/100 g was measured at pH 4. The imogolite surface charge was estimated at one positive charge per 700 Å<sup>2</sup>, or one

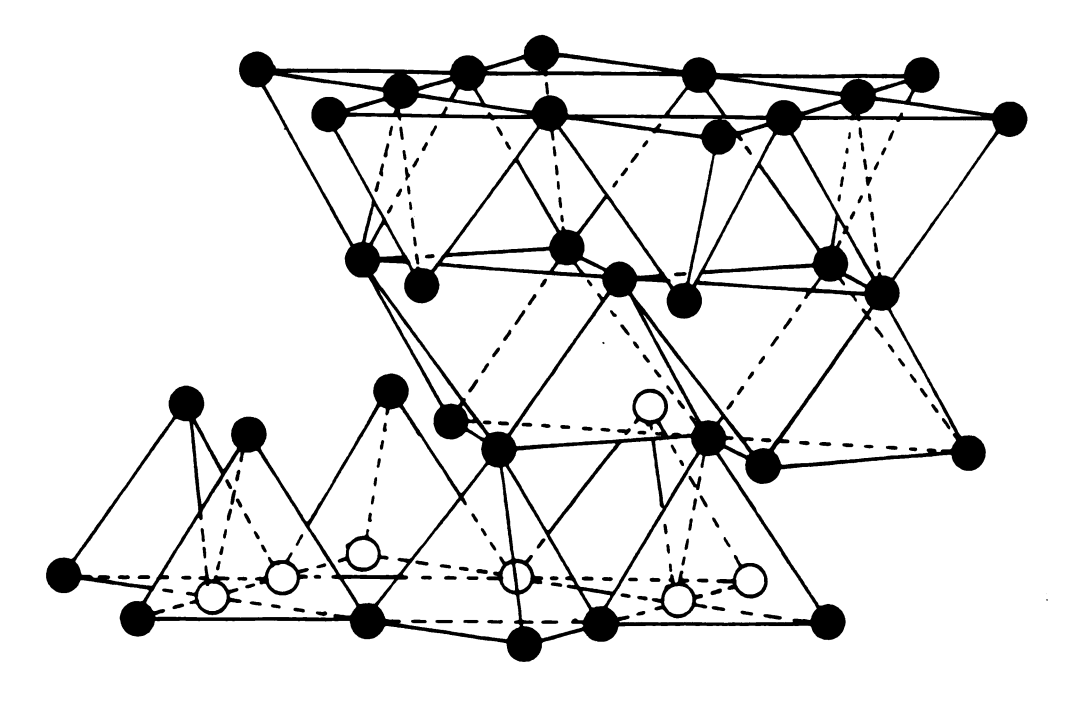
positive charge per 40 aluminum. Phosphate adsorption onto imogolite was also determined. The capacity of imogolite to adsorb phosphate was only 12 meq/100 g, much lower than that of chloride. Phosphate was presumed to adsorb to defect sites or  $Al(OH)H_2O$  sites at the tube edges more readily than external Al-OH-Al sites, resulting in a reduced adsorption capacity.

Clark and McBride<sup>13</sup> also measured chloride adsorption as a function of pH. Results obtained from positive surface charge measurements on imogolite using NaCl differed from those obtained using NaClO4. Adsorption capacities obtained from measurements of negative surface charge were independent of adsorbate. Anion dependent intercalation of the neutral salts was proposed to explain the anomalous results. In a separate paper, Clark and McBride 14 reported obtaining anomalous results from experiments involving the adsorption of Cu(II) and Co(II) onto imogolite. The amount of Cu(II) adsorbed as a function of the concentration of Cu cations in solution, approached a plateau at a much lower value than the corresponding Co(II) adsorption curve. Again, it was necessary to consider intercalation of  $Cu(NO_3)_2$  ion pairs to explain the anomaly. The solution stability of the cupric nitrate ion pairs is much greater than the stability of the corresponding cobalt nitrate ion pairs in solution. Therefore, intercalation effects were only observed for Cu ion adsorption. The potential for imagolite to intercalate

neutral ion pairs should be recognized when imagolite interacts with charged species.

#### C. Na-MONTMORILLONITE

Na-montmorillonite clay was used to improve the performance of imogolite as a catalyst material, and to aid characterization of surface modified imogolite The layered structure of Na-montmorillonite products. coupled with its capacity to undergo ion exchange makes this clay mineral ideal for these applications. The idealized structure of Na-montmorillonite is shown in Figure I.2. The idealized chemical formula for montmorillonite is  $M^{n+}_{x/n}$  ·yH<sub>2</sub>O[Al<sub>4-x</sub>Mg<sub>x</sub>](Si<sub>8</sub>)O<sub>20</sub>(OH)<sub>4</sub>. layer is composed of four planes of oxygens which define upper and lower sheets of tetrahedral sites and a central sheet of octahedral sites. This 2:1 ratio of tetrahedral to octahedral sheets classifies Na-montmorillonite as a 2:1 phyllosilicate. Pinnavaia 15 provides an excellent review of the structure, properties and classifications of clay minerals. The cation exchange properties of montmorillonite clay arise from the presence of hydrated exchangeable cations between the clay layers. These interlayer cations balance the net negative charge on the clay layer, originating from the substitution of octahedral  $Al^{3+}$  by  $Mq^{2+}$ . Imagolite and surface modified imagolite, having a net surface positive charge, can be intercalated between the layers of Na-montmorillonite through the



 $M^{n+} \cdot xH_2O$ 

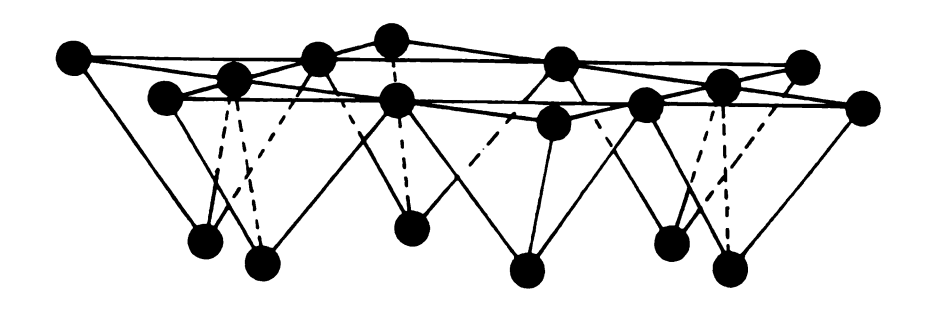


Figure I.2. Idealized structure of Na-montmorillonite. Silicon atoms occupy the tetrahedral positions in the oxygen framework, aluminum or magnesium atoms occupy the octahedral sites.  $\mathbf{M}^{\mathbf{N}^+}$  represents the interlayer Na cation.

replacement of the hydrated Na cations. The identification of surface-modified imagolite intercalated montmorillonite reaction products may aid in the characterization of surface-modified imagolite reaction products.

#### D. TUBULAR SILICATE LAYERED SILICATE, TSLS

The utility of imogolite as a catalyst material was compromised by an unfavorably low dehydroxylation onset temperature of 350°C. The resistance of the tubular structure to dehydroxylation has been improved by the intercalation of the individual imogolite tubes as regular monolayer between the layers of Na-montmorillonite clav. 16 Dehydroxylation of the tubular silicate layered silicate, or TSLS complex, is initiated at >400°C. TSLS material consists of aligned rows of imogolite tubes in van der Waals contact with adjacent tubes along the length of the interlayer and with the clay layer in the direction perpendicular to the interlayer. This illustrated schematically in Figure I.3. The microporosity observed for this material is therefore limited to the channels within the tubes, and the pores formed by packing the cylinders against planar sheets. 17

#### E. RESEARCH OBJECTIVES

The goal of this work was catalyst design; increasing the microporosity of the pillared clay catalyst material, TSLS, through surface modification of the imagolite pillar

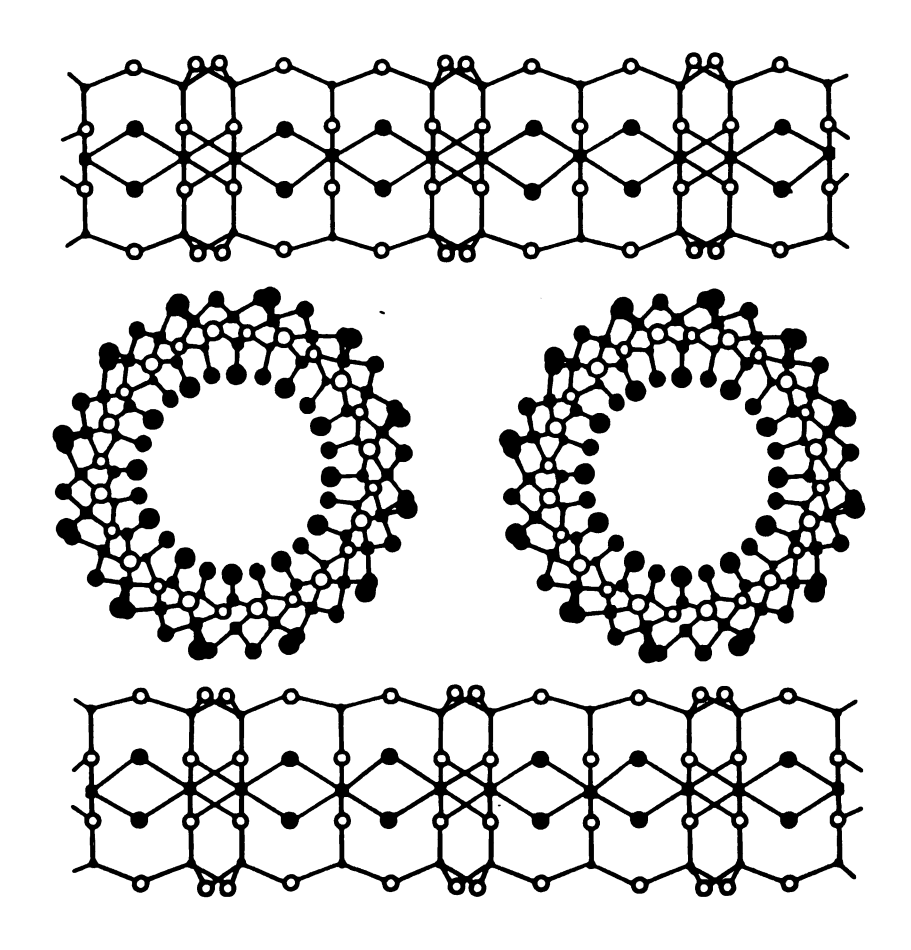


Figure I.3. Schematic representation of TSLS.

prior to intercalation. Controlled absorption of coupling agent to the external surfaces of imogolite as a regular monolayer, was envisioned to introduce bulk between the individual tubular units, forcing lateral separation between the tubes surface-modified-imogolite in a intercalated Na-montmorillonite product. Removal of the surface modifying agent by calcination, might introduce permanent porosity between the imogolite tubes.

The absence of van der Waals contact between neighboring tubes in the surface-modified-imogolite intercalated material may result in reduced dehydroxylation onset temperatures for the new material. A superior catalyst material might still be isolated from the high temperature decomposition products of imogolite. The decomposition mechanism proposed by MacKenzie et al., 18 suggests that the individual imogolite tubes would undergo cleavage of the oxygen linkages along their midsection, followed by subsequent flattening and condensation of the two fragments. Decomposition of laterally separated, Namontmorillonite intercalated imogolite tubes in this way, might result in a layered aluminosilicate pillared smectite Consequently, the calcined product of laterally imogolite within the galleries montmorillonite might lead to the formation of an entirely new microporous material.

#### F. APS-MODIFIED IMOGOLITE/Na-MONTMORILLONITE

Surface modification of imogolite was first attempted using a 2 wt. % solution of the coupling agent gammaaminopropyltriethoxysilane (APS). The behavior of this coupling agent in solution and its interaction hydroxylated surfaces has been previously described. 11 Several criterion must be satisfied in order for a surface modified imogolite to perform as envisioned. Most importantly, a net positive charge must be retained to avoid aggregation of the tubes. This requires a reaction pH no greater than 7 and an imagolite concentration <0.4 wt. %. APS was attractive as a potential surface modifying agent because of its ability to uniformly couple to hydroxylated surfaces. This behavior is promoted by APS hydrolysis at concentrations of 2 wt. % at pH 4 in aqueous solution because the hydrolyzed APS exists in chiefly monomeric form the trisilanol). Under (as conditions, the aminofunctionality is protonated, promoting coupling between the silanol groups and the positively charged imagolite surface. APS coupled to imagolite in this way would maintain a positive surface charge, enabling intercalation of the surface coupled products into the galleries of the Na-montmorillonite clay. .

Gamma-ammoniumpropylsiloxane polymer coupling to the imogolite surface was confirmed by <sup>29</sup>Si MAS NMR and Fourier Transform Infrared spectroscopy (FTIR) from air-dried products obtained by treating 0.1 wt. % imogolite

suspensions with 2 wt. % APS solutions hydrolyzed at pH 3.6 in the presence of acetic acid. 19 The hydrolytic instability of the APS-modified imogolite products was subsequently demonstrated by depletion of the organosiloxane polymer from suspensions of APS-modified imogolite during dialysis against deionized water. The APS depletion rate was determined by monitoring the concentration of the air-dried products by FTIR at intervals throughout dialysis.

The isolation of APS-modified imogolite intercalation products might have been possible despite the somewhat labile nature of the imogolite-polymer interface. Intercalation of the imogolite tubes was known to be rapid, and the interaction between the clay layers and the APSmodified imogolite could have had a stabilizing effect on the complex. Attempts to intercalate APS-modified imogolite between the layers of Na-montmorillonite clay unsuccessful. The reaction products reflected the dynamic nature of the APS-coupled imogolite material.

#### G. PHOSPHORUS ACID COUPLED ALUMINA SURFACES

Phosphonic acids were selected as surface modifying agents in an effort to obtain a surface modified imogolite product with increased stability. Phosphonic acids have been successfully coupled to alumina surfaces from aqueous solution. The adsorption of phosphorus acids on alumina

has shown to provide increased resistance to corrosion. Surface coupling between phosphorus acids and alumina has been characterized by Infrared (IR), Inelastic Electron Tunneling (IET) and Auger Electron spectroscopy.

Ramsier et al. $^{20}$  studied the adsorption from aqueous solution of several phosphorus acids [phosphonic acid (PA), phosphinic acid (PPA), hydroxymethyl phosphonic acid (HMPA) nitrilotris(methylene)-triphosphonic acid  $(N[CH_2P(O)(OH)_2]_3)$ ] on alumina by IR and IETS. The absence of P=O bands in the spectra of the adsorbed species led to the conclusion that these acids were chemisorbed to the alumina surface through resonance stabilized structures of a symmetric phosphonate (phosphinate) group. The presence of P-H bands in the spectrum of the adsorbed NTMP, however, suggested that this acid dissociates upon adsorption by P-C and C-N bond cleavage. The PA and HMPA decomposition byproducts of the NTMP were adsorbed to the alumina surface while the amine and alcohol decomposition byproducts were evolved as gases.

Weinberg<sup>21,22</sup> have identified Templeton and temperature dependent molecular and dissociative adsorption pathways in gas phase adsorption studies of phosphonate esters on alumina. Dimethyl methylphosphonate (CH<sub>3</sub>O)<sub>2</sub>(CH<sub>3</sub>)P(O), DMMP, dissociates through P-O bond cleavage to form the methyl methylphosphonate species which adsorbs to the alumina surface through its two remaining P-O units.

White et al. $^{23}$  and Davis et al. $^{24}$  addressed the relationship between the ability of phosphorus acids to adsorb to alumina surfaces and the corrosion resistance performance of the phosphorus acid-coupled material. White et al. utilized IETS, FTIR and molecular electrostatic potential calculations to determine the relative strengths of adsorption of PA, HMP, MPA and NTMP on alumina. were able to correlate the best hydration inhibitor, NTMP, with the strongest adsorption and the poorest hydration inhibitor, MPA, with the weakest adsorption. Davis et al. 24 examined the IET spectra of NTMP adsorbed onto aluminum coupons from aqueous solution. adsorption occurred by the stepwise displacement of water or hydroxyl groups on the surface by the phosphonate 'legs' of the NTMP. Davis et al. also monitored the surface of the NTMP-coupled aluminum coupons during exposure to humidity in an effort to understand the corrosion process. Corrosion was also found to be a stepwise process, initiated by the slow dissolution of the NTMP from the surface and followed by the rapid hydration/corrosion of the freshly exposed aluminum.

#### H. APP-MODIFIED IMOGOLITE/Na-MONTMORILLONITE

Gamma-aminopropylphosphonic acid (APP), the phosphonic acid analog to APS, was chosen for its ability to preferentially orient itself with respect to the imagolite surface to maintain a positive surface charge in the pH

The species exists as a neutral range of interest. zwitterion +NH<sub>3</sub>(CH<sub>2</sub>)<sub>3</sub>PO<sub>3</sub>H in the solid state, determined from x-ray crystallography. 25 In solution, the relative concentrations of APP species are dictated by three acid dissociation constants. Appleton et al.<sup>26</sup> determined the effect of pH on the 31p and 1H NMR spectra various aminoalkylphosphonic acids in including APP. FTIR has also played an important role in structural identification of the phosphonic Diagnostic IR bands allowing differentiation between APP species in solid samples have been assigned by Garrigou-Lagrange et al.<sup>27</sup> among others.<sup>28-31</sup>

surface coupled products obtained from the reaction of imogolite with APP at 0.43:1 APP:imogolite at pH 7.5 and pH 3.5 have been characterized by 31P MAS NMR and FTIR. The well-ordered products obtained by reaction of Na-montmorillonite with 5.9 moles APP/clay equivalent at pH 3.9 and 7.5 have also been characterized by x-ray diffraction, elemental analysis and <sup>31</sup>P NMR, in order to distinguish them from APP-modified imogolite intercalation products. The ordered products obtained from the reaction of APP-modified imagolite at pH 7.5 and 0.43:1 (w/w) APP:imogolite with Na-montmorillonite at 2.5:1 (w/w) unmodified imagolite to clay after one washing have also been analyzed. The ordered products isolated were not the expected APP-modified imogolite intercalated complexes.



#### LIST OF REFERENCES

- Handbook of Chromatography, V. 2; Zweig, G.; Sherma,
   J., Eds.; CRC Press: Cleveland, OH, 1972.
- 2. Pines, H.; Haag, W. J. Am. Chem. Soc. 1960, 82, 2471.
- 3. Maciver, D.S.; Tobin, H.H.; Barth, R.T.; J. Catalysis 1963, 2, 485.
- 4. Peri, J.B.; Hannan, R.B. J. Phys. Chem. 1960, 64, 1526.
- 5. Peri, J.B. J. Phys. Chem. 1965, 69, 211.
- 6. Peri, J.B. J. Phys. Chem. 1965, 69, 220.
- 7. Cradwick, P.D.G.; Farmer, V.C.; Russell, J.D.; Masson, C.R.; Wada, K.; Yoshinaga, N. Nature Phys. Sci. 1972, 240, 187.
- 8. Farmer, V.C.; Fraser, A.R. Dev. Sedimentol. 1978, 27, 547.
- 9. Barron, P.F.; Wilson, M.A.; Campbell, A.S.; Frost, R.L. Nature 1982, 299, 616.
- 10. Goodman, B.A.; Russell, J.D.; Montez, B.; Oldfield,
  E.; Kirkpatrick, R. J. Phys. Chem. Miner. 1985, 12,
  342.
- 11. Johnson, L.M. M.S. Thesis, Michigan State University, 1988.
- 12. Theng, B.K.G.; Russell, M.; Churchman, G.J.; Parfitt, R.L. Clays Clay Miner. 1982, 30, 143.
- 13. Clark, C.J.; McBride, M.B. Clays Clay Miner. 1984, 32, 291.
- 14. Clark, C.J.; McBride, M.B. Clays Clay Miner. 1984, 32, 300.
- 15. Pinnavaia, T.J. Science 1983, 220, 365.
- 16. Johnson, I.D.; Werpy, T.A.; Pinnavaia, T.J. J. Am. Chem. Soc. 1988, 110, 8545.

- 17. Werpy, T.A.; Michot, L.J.; Pinnavaia, T.J. In Novel Materials in Heterogeneous Catalysis; Baker, R.T.K.; Murrell, L.L., Eds.; American Chemical Society: Washington, D.C., 1990.
- 18. MacKenzie, K.J.D.; Bowden, M.E.; Brown, I.W.M.; Meinhold, R.H. Clays Clay Miner. 1989, 37, 317.
- 19. Johnson, L.M.; Pinnavaia, T.J. Langmuir 1990, 6, 307.
- 20. Ramsier, R.D.; Henriksen, P.N.; Gent, A.N. Surf. Sci. 1988, 203, 72.
- 21. Templeton, M.K.; Weinberg, W.H. J. Am. Chem. Soc. 1985, 107, 97.
- 22. Templeton, M.K.; Weinberg, W.H. J. Am. Chem. Soc. 1985, 107, 774.
- 23. White, H.W.; Crowder, C.D.; Alldredge, G.P. J. Electrochem. Soc. 1985, 132, 773.
- 24. Davis, G.D.; Ahearn, J.S.; Venables, J.D. J. Vac. Sci. Technol. 1984, A2, 763.
- 25. Glowiak, T.; Sawka-Dobrowolska, W. Acta. Cryst. 1980, B36, 961.
- 26. Appleton, T.G.; Hall, J.R.; Harris, A.D.; Kimlin, H.A.; McMahan, I.J. Aust. J. Chem. 1984, 37, 1833.
- 27. Garrigou-Lagrange, C.; Destrade, C. J. Chim. Phys. 1970, 67, 1646.
- 28. Destrade, C.; Garrigou-Lagrange, C. J. Chim. Phys. 1970. 67, 2013.
- 29. Menke, A.G.; Walmsley, F. Inorg. Chim. Acta 1976, 17, 193.
- 30. Fenot, P.; Darriet, J.; Garrigou-Lagrange, C.; Cassaigne, A. J. Mol. Struct. 1978, 43, 49.
- 31. Sahni, S.K.; van Bennekom, R.; Reedijk, J. Polyhedron 1985, 4, 1643.

#### CHAPTER II

Silylation of a Tubular Aluminosilicate Polymer (Imogolite), by Reaction with Hydrolyzed gamma-aminopropyltriethoxysilane (APS)

#### A. INTRODUCTION

Chemical modification of surfaces is an area of intense interest from both fundamental and practical points of view. 1-5 A variety of analytical techniques which have been recently developed enable the surface chemical interactions to be studied and the chemical species present on a surface to be identified. 6-9 This molecular-level information is essential for an understanding of the macroscopic properties of a surface, such as adhesion, resistance to chemical attack, and fracture.

The tubular aluminosilicate polymer imogolite,  $(HO)_3Al_2O_3Si(OH)$ , targeted has been for modification in the present study. The imagolite structure is shown in cross-section in Figure II.1. The molecular size of the tubular unit (-23 Å diameter, -8 Å internal channel and 250 - 350 nm length) gives rise to a large surface area of  $900 \text{ m}^2/\text{g.}^{10}$ The hydroxylated external surface imparts water solubility to the tubes at low concentration (< 0.4 wt. %) and acidic pH. Treatment of the hydroxylated surfaces with organosilanes may allow for a more hydrophobic surface, permitting extraction of the tubular units into organic solvents. The ability to control the solubility properties of imogolite using surface modification techniques could lead to broader

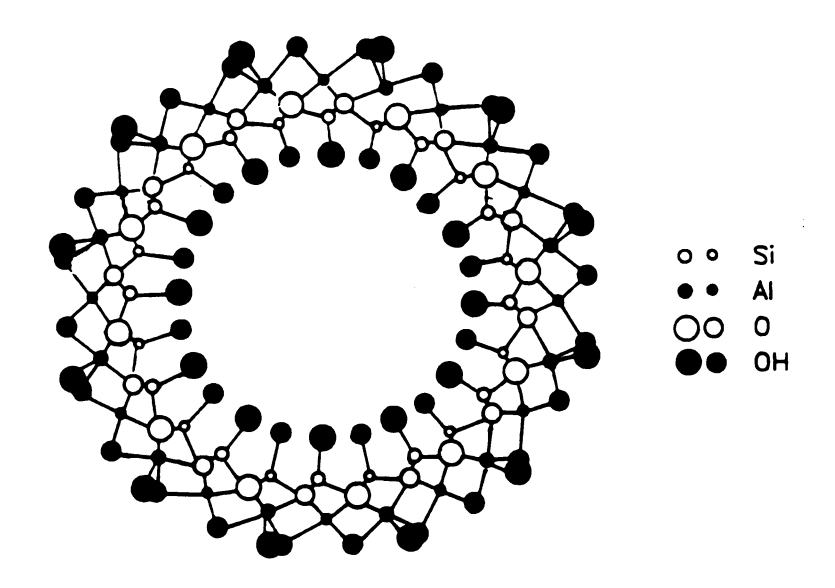


Figure II.1. Cross-sectional view of the tubular aluminosilicate imogolite (adapted from reference 22). The inner and outer tube diameters are -8.2 Å and 23 Å, respectively. Tube lengths of the synthetic derivative used in the present work are typically from 250 to 350 nm. The empirical formula, as read from outer to inner atomic planes is  $(HO)_3Al_2O_3Si(OH)$ .

applications of this novel inorganic polymer in materials science.

The reaction of imogolite with hydrolyzed gamma-aminopropyltriethoxysilane (APS) was investigated as a means of achieving the desired surface modification, in part, because of the proven utility of hydrolyzed APS for the organofunctionalization of inorganic oxide surfaces. 11,12

#### B. EXPERIMENTAL

Imogolite was synthesized according to the method described by Farmer and Fraser<sup>13</sup> and purified by dialysis against deionized water. The hydrolyzed APS-imogolite products were prepared by addition of a 2 wt. % aqueous APS solution to a 0.1 wt. % suspension of purified imogolite with subsequent stirring overnight. The 2 wt. % hydrolyzed APS solution was prepared by reaction of APS (Petrarch Systems) with water over a period of half an hour in the presence of enough acetic acid to achieve a pH of 3.6. low pH is desirable for the coupling reaction because under conditions imogolite remains these soluble and APS undergoes rapid and complete hydrolysis. The amount of APS incorporated in the coupling reaction was based on the amount of aluminum used in the imogolite synthesis. the synthesis of imogolite is not quantitative, typically in < 50 % yield, the amount of APS present in the coupling reaction was always in excess of monolayer coverage, even

when the formal APS: Al ratio was at the lowest formal value of 0.5: 1.0.

FTIR vibrational spectra for KBr-pellet samples were obtained on an IBM model IR40S spectrometer equipped with IR44 work station. an IBM Difference spectra imogolite-bound APS were obtained by weighted digital subtraction of the imogolite spectrum from the spectra of the APS-imogolite reaction products. Subtractions were performed over the frequency range 4000 cm<sup>-1</sup> to 400 cm<sup>-1</sup>. Baseline corrections were not needed. Spectra generated in transmittance mode gave difference spectra in agreement  $(\pm 2 \text{ cm}^{-1})$  with those generated in absorbance mode. validity of the difference routine was checked by comparing the difference spectrum for APS on APS-modified silica gel with the difference spectrum reported by Chiang et al. 14 spectral resolution Within the of our instrument  $(\pm 2 \text{ cm}^{-1})$ , the frequencies obtained for our difference spectrum were identical to those obtained by Chiang et al.

<sup>29</sup>Si MAS NMR spectra were obtained at 35.76 MHz on a Bruker WH-180 spectrometer equipped with a Doty magic angle spinning probe.

# C. RESULTS

When hydrolyzed APS was mixed with imogolite at pH 3.6, there was no visible indication of reaction. Both reaction components remain dissolved and the reaction mixture remained colorless. An initial attempt to separate

silylated imogolite from unreacted APS by dialysis was inconclusive, because of the hydrolytic instability of the silylated imogolite products. Complete and facile removal of the coupling agent was achieved after three days of dialysis at room temperature. Despite the hydrolytic instability of the system, FTIR and MAS <sup>29</sup>Si NMR experiments demonstrated that there is indeed binding between the hydrolyzed APS and imogolite and that the resulting products are not simply homogeneous mixtures of the two reaction components.

Shown in Figure II.2A is the FTIR spectrum of APS polymer prepared by air-drying a film on a glass slide. The spectrum in Figure II.2B represents air-dried APS which has been hydrolyzed in the presence of acetic acid at pH 3.6. The pair of bands near 1130  $cm^{-1}$  and 1030  $cm^{-1}$  in both spectra are assigned to the asymmetric stretching frequencies of Si-O-Si linkages in the polymer. observed frequencies of the bands in the 1300 cm<sup>-1</sup> to 1600 cm<sup>-1</sup> region reflect both the nature of the counter ion associated with the protonated aminofunctionality and the degree of protonation resulting from the hydrolysis conditions. The partially protonated aminosilane polymer formed by hydrolysis of APS in air exhibits carboxylate stretching frequencies characteristic of bicarbonate ions  $[v_{as}(CO_2^{-}), 1638 \text{ cm}^{-1}; v_{s}(CO_2^{-}), 1336 \text{ cm}^{-1}]^{15}$  in addition to onium ion stretching frequencies [vas(NH3+), 1580 cm-1;  $v_s(NH_3^+)$ , 1484 cm<sup>-1</sup>] in accord with earlier assignments for

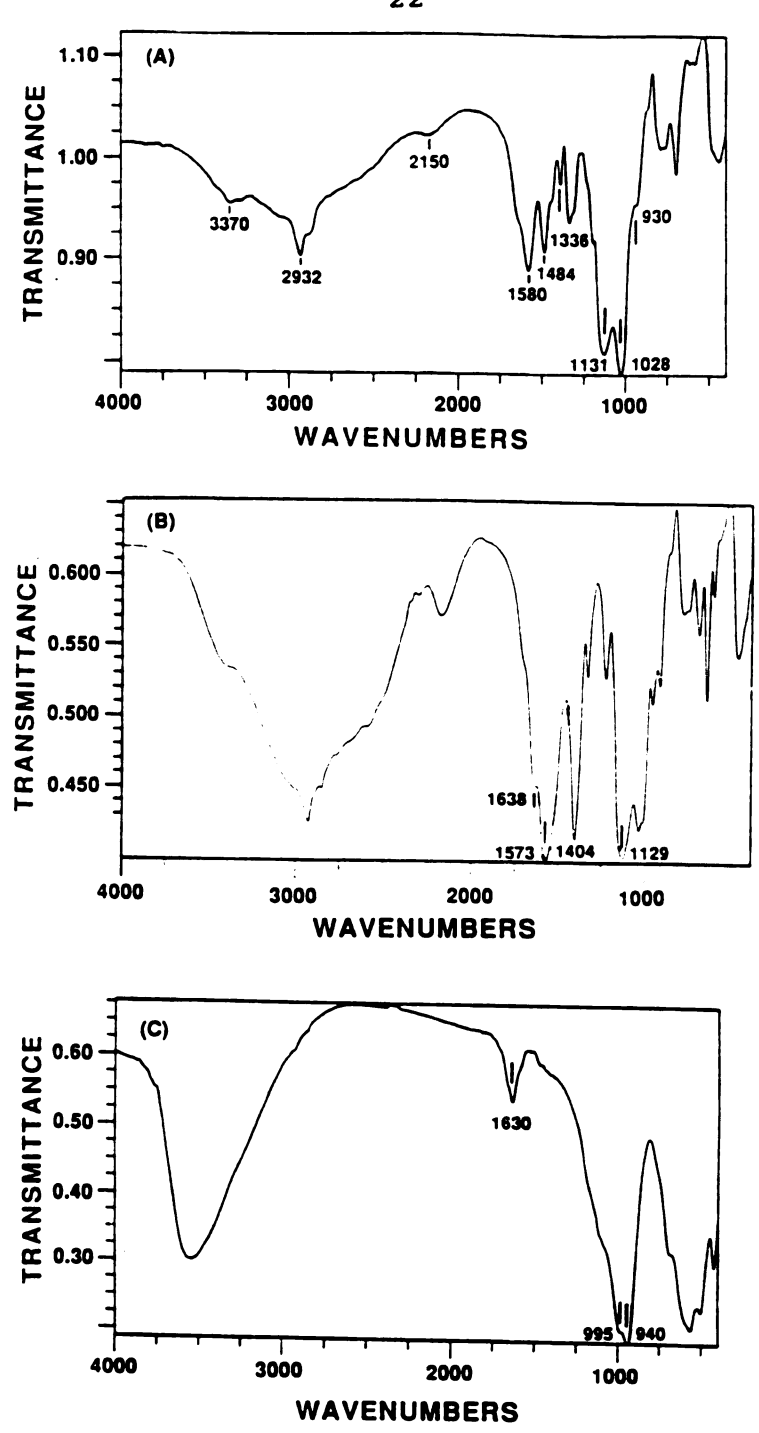
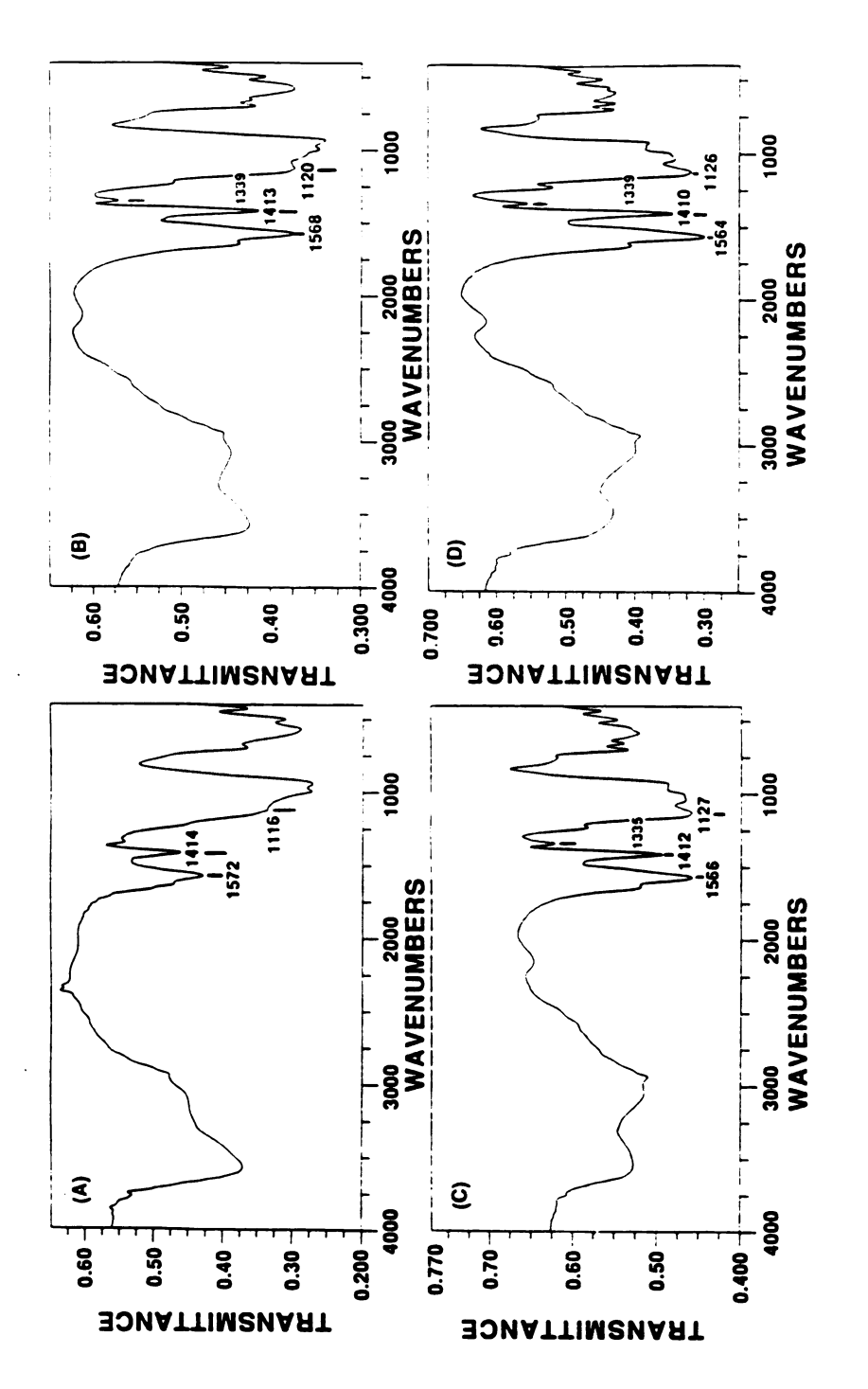


Figure II.2. FTIR spectra (KBr disks) of (A) APS polymer prepared by hydrolysis and drying in air; (B) APS polymer prepared by hydrolysis in acetic acid at pH 3.6 and air drying; and (C) synthetic imagolite.

the hydrolyzate of APS at ambient pH.  $^{14,16-18}$  The poly-(gamma-ammoniumpropyl) siloxane acetate formed by hydrolysis of APS in the presence of aqueous acetic acid, however, in addition to  $[v_{as}(NH_3^+), 1573 \text{ cm}^{-1}]$  exhibits characteristic bands due to the presence of both bicarbonate  $[v_{as}(CO_2^-), 1638 \text{ cm}^{-1}; v_{s}(CO_2^-), 1336 \text{ cm}^{-1})$  and acetate  $[v_{s}(CO_2^-), 1404 \text{ cm}^{-1}; \delta(OCO), 653 \text{ cm}^{-1}]$  19 counter ions.

The FTIR spectrum of imogolite shown in Figure II.2C is characterized by the presence of prominent water bands near 3500 cm<sup>-1</sup> due to the OH stretch and near 1630 cm<sup>-1</sup> due to the HOH bending vibration. The two bands located at 995 cm<sup>-1</sup> and 940 cm<sup>-1</sup> are those characteristic of the Si-O-Al stretching vibrations of the tubular silicate.<sup>20</sup> These latter bands are consistent with the presence of grafted orthosilicate units in imogolite.

The FTIR spectra of the hydrolyzed APS-imogolite reaction products contain several interesting features. Figure II.3 provides the spectra of the products obtained at formal APS: Al mole ratios of 0.5:1,1:1,2:1 and 2.5:1. The position of the  $v_{as}(\mathrm{NH_3}^+)$  frequencies  $(1564-1572~\mathrm{cm}^{-1})$  and  $V_{s}(\mathrm{CO_2}^-)$  frequencies  $(1410-1414~\mathrm{cm}^{-1})$  are similar to those observed in the pure polymer formed by acid hydrolysis  $(1573~\mathrm{and}~1404~\mathrm{cm}^{-1})$ , respectively). Two  $v_{as}(\mathrm{Si-O-Si})$  bands  $^{14}$  due to the coupling agent are found above  $1000~\mathrm{cm}^{-1}$ ; one band occurs at  $1130~\mathrm{cm}^{-1}$  and the other occurs at  $1030~\mathrm{cm}^{-1}$ . These

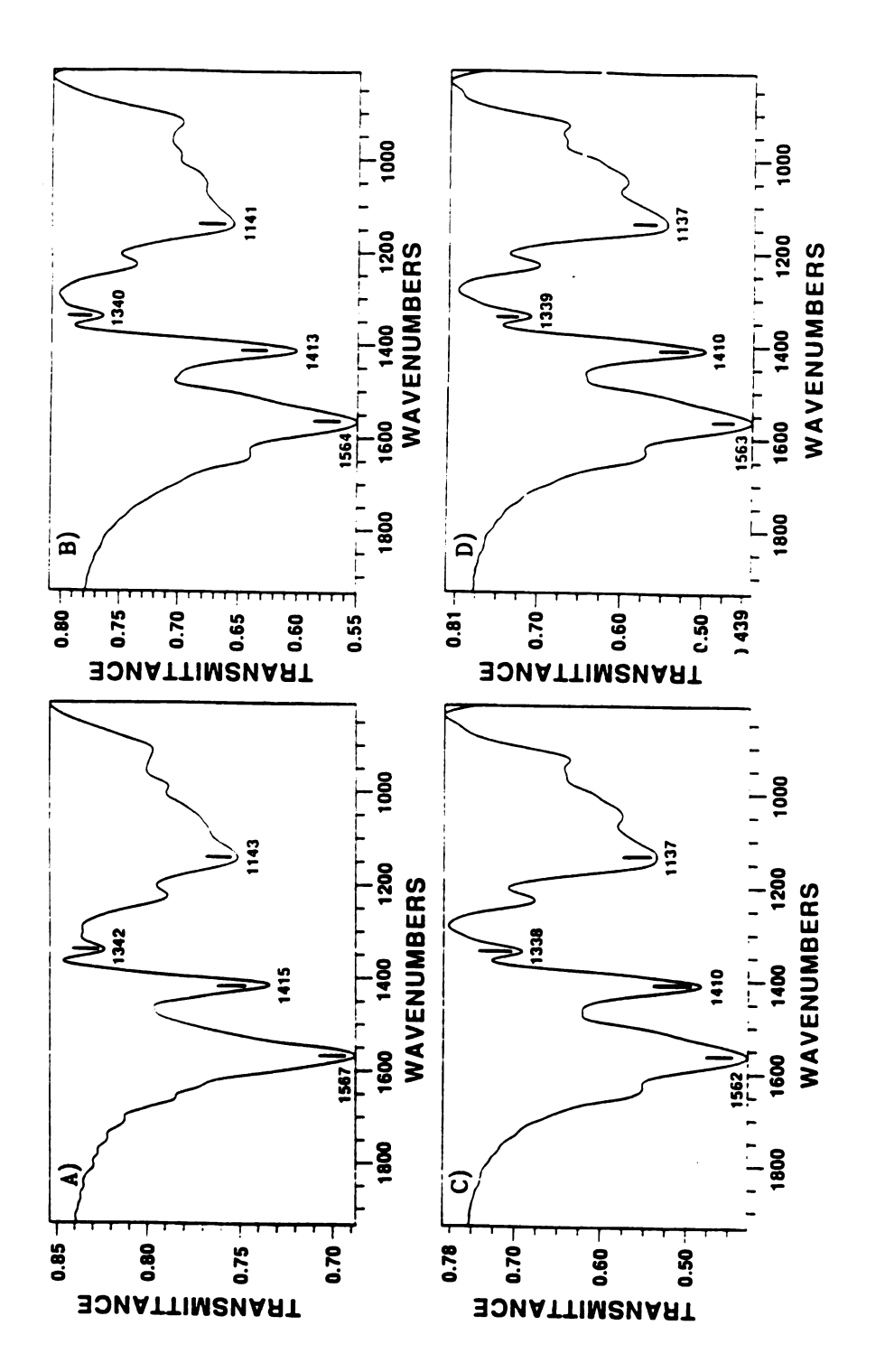


silylated: Al molar imogolite reaction products formed at spectra (B) FTIR (A) 0.5Figure II.3. ratios of

bands are more easily observed in the spectra of products containing higher APS concentrations. The assignment of these two bands to mainly Si-O-Si stretch frequencies is consistent with the presence of a network of highly polymerized silane covering the imagolite tubes. A monolayer of APS monomers and dimers linked to the surface should have been represented by a single band near  $1016 \text{ cm}^{-1}.14$ 

It was desirable to obtain further evidence for a coupling reaction between the hydrolyzed APS and imogolite, and to eliminate the possibility that the observed spectra may be due to a physical mixture of imogolite and APS polymer. This was accomplished through the analysis of difference spectra obtained by digital subtraction of the imogolite spectrum (cf., Figure II.2C) from spectra obtained for the reaction products in Figure II.3. The difference spectra are shown in Figure II.4.

The region between  $1600 \text{ cm}^{-1}$  and  $1100 \text{ cm}^{-1}$  in the difference spectra is of special interest. The band in the  $1129 - 1143 \text{ cm}^{-1}$  region is an asymmetric Si-O-Si stretch arising from the self-condensation of hydrolyzed APS units. Since imagolite does not contain siloxane bonds, the Si-O-Si stretch in the silylated reaction products arises exclusively from the surface-bound polymer. In the four resultant spectra this band is shifted to lower wavenumbers with increasing concentration of APS. The positions of other bands such as  $v_{as}(\text{CO}_2^{-1})$  and  $v_{s}(\text{CO}_2^{-1})$  due to



FTIR difference spectra for the region between 2000 cm<sup>-1</sup> obtained by digital subtraction of spectrum in Figure II.2C from the spectra for the imogolite spectrum in Figure II.2C from the sp the APS-imogolite reaction products in Figure II.3. Figure II.4 800 cm-1

bicarbonate ion and  $v_s({\rm CO}_2^-)$  due to acetate ion remain unshifted in the difference spectra.

Table II.I lists the relevant FTIR frequencies observed for the reaction products obtained at different APS: Al molar ratios. The frequencies for the airhydrolyzed and acid-hydrolyzed APS polymer as an isolated solid are also included. The 14 cm<sup>-1</sup> shift in  $V_{as}(Si-O-Si)$ from 1129 cm<sup>-1</sup> in the pure acid hydrolyzed polysiloxane to 1143  $cm^{-1}$  in the 0.5 : 1.0 APS : Al reaction product is significant. Although the 14 cm<sup>-1</sup> shift is deduced from difference spectra, the magnitude of the shift is much larger than the 2.0 cm<sup>-1</sup> instrumental resolution. A shift in this band is also observed in the unsubtracted spectra as shown in Table II.I, but in the opposite direction. This is due to the fact that, especially at low APS concentrations, the band position is shifted interference from the broad imagolite Si-O-Al band. (cf., Figures II.3A and II.3B.)

<sup>29</sup>Si MAS NMR spectroscopy was used to further probe this system in an effort to obtain additional insights into the nature of APS bound to imogolite. Pure synthetic imogolite exhibits a single resonance at -79 ppm, in agreement with the shift reported for naturally occurring imogolite. <sup>21,22</sup> As shown in Figure II.5A, a single resonance due to fully cross-linked RSi(OSi)<sub>3</sub> sites is observed for acid-hydrolyzed APS, <sup>23</sup> but the siloxane line occurs at -69 ppm, about 10 ppm downfield from imogolite.

Table II.I. FTIR vibrational frequencies (cm<sup>-1</sup>) for hydrolyzed APS and hydrolyzed APS-imogolite reaction products.<sup>a</sup>

Formal APS : Al Ratio	$v_{as}(NH_3^+)$	v <sub>s</sub> (CO <sub>2</sub> )	$v_s(CO_2)$	v <sub>as</sub> (SiOSi)
		Unsubtracte	ed Spectra	
1.0 : 0.0d	1580	-	1336	1131
1.0 : 0.0e	1573	1404	1336	1129
2.5 : 1.0	1564	1410	1339	1126
2.0 : 1.0	1566	1412	1335	1127
1.0 : 1.0	1568	1413	1339	1120
0.5 : 1.0	1572	1414	1342	1116
		Subtracted	Spectra	
2.5 : 1.0	1563	1410	1339	1137
2.0 : 1.0	1562	1410	1338	1137
1.0 : 1.0	1564	1413	1340	1141
0.5 : 1.0	1567	1415	1342	1143

<sup>&</sup>lt;sup>a</sup> All reactions were carried out in aqueous acetic acid at pH 3.6 except where otherwise indicated.

b This is the symmetric carboxylate stretching frequency of the acetate counter-ion.

<sup>&</sup>lt;sup>C</sup> This is the symmetric carboxylate stretching frequency of the bicarbonate counter-ion.

d This ratio is representative of the pure APS polymer formed by hydrolysis and drying in air.

<sup>&</sup>lt;sup>e</sup> This ratio is representative of the pure APS polymer formed by hydrolysis in acetic acid solution at pH 3.6 and subsequent evaporation in air.

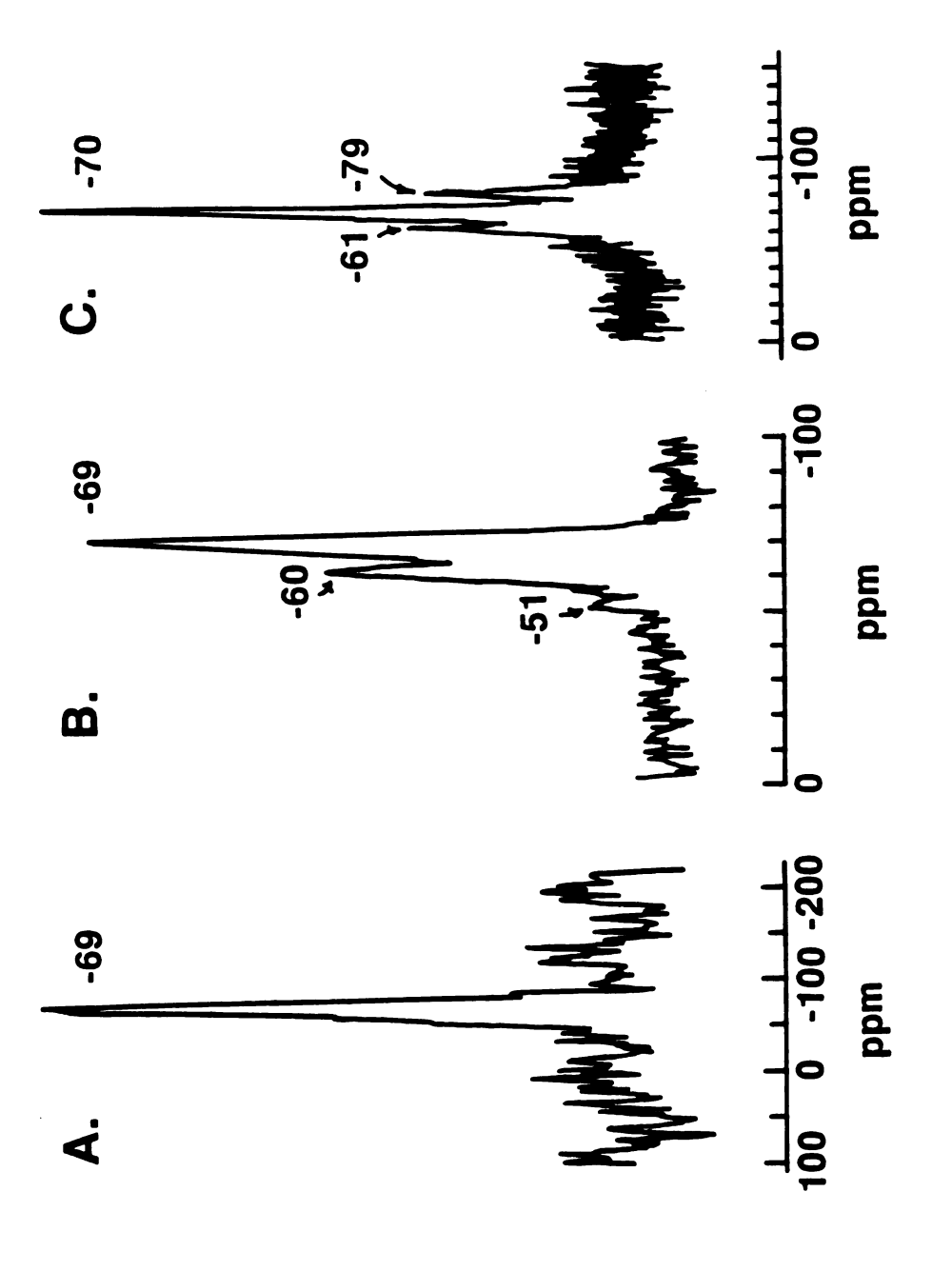


Figure II.5. <sup>29</sup>Si MAS NMR spectra: (A) the pure siloxane polymer obtained by hydrolysis in aqueous acetic acid at pH 3.6; (B) the pure siloxane polymer obtained by hydrolysis in water; (C) the acid-hydrolyzed APS-imogolite reaction product obtained at a formal APS: Al ratio of 0.5: 1.0.

This chemical shift difference readily distinguishes the silicon environments in imogolite and hydrolyzed APS. Interestingly, if pure APS is hydrolyzed in water rather than in aqueous acetic acid, then three resonances are observed as shown in Figure II.5B. We assign the lines at -69, -60, and -51 ppm to RSi(OSi)<sub>3</sub>, RSiX(OSi)<sub>2</sub>, and RSiX<sub>2</sub>(OSi) end groups, respectively, where X represents an -OH or, less likely, an unhydrolyzed -OC<sub>2</sub>H<sub>5</sub> group. These assignments are in agreement with those given by Caravajal<sup>24</sup> et al., among other workers.<sup>23,25-26</sup>

Figure II.5C illustrates the <sup>29</sup>Si MAS NMR spectrum of the imagolite-APS reaction product obtained at a formal APS:Al ratio of 0.5 : 1.0. At this reaction ratio, the APS is in excess of ideal monolayer coverage, as judged by the of the siloxane relative intensities and imogolite resonances. The line at -80 ppm corresponds to the  $Q^3(3A1)$ environment of imogolite. Significantly, the organosilane region exhibits two silicon resonances at -70 and -61 ppm. Since <sup>29</sup>Si chemical shifts of siloxanes move upfield with increasing degree of cross-linking to neighboring silicon sites, we attribute the -70 ppm resonance to a fully crosslinked RSi(OSi)3 site analogous to that in pure acidhydrolyzed APS, whereas the -61 ppm line is assigned to a less cross-linked RSiX(OSi)<sub>2</sub> environment.

#### D. DISCUSSION

The hydrolysis of APS in acidic aqueous solution (pH 3.6) is known to afford mainly monomer and dimer species. Thus, the silanol is much more stable toward self-condensation to higher molecular weight polysiloxanes than other organosilanes. The solution stabilization is thought to be due to an interaction between the aminofunctional group and either the silicon center or the hydrogen of one of the silanols. 14,27-29 This interaction protects the silanols against further condensation and inhibits polymerization. 29

limited condensation of The silanols between units prevents precipitation hydrolyzed APS of organosilane coupling agent from solution. But the evaporation at room temperature of an hydrolyzed APS solution containing acetic acid at pH 3.6 does result in the formation of a siloxane polymer, as indicated by the appearance of siloxane stretching frequencies at 1129 cm<sup>-1</sup> and 1035 cm<sup>-1</sup> (cf. Figure II.2B) and in the appearance of only fully cross-linked RSi(OSi)<sub>3</sub> sites in the <sup>29</sup>Si MAS NMR spectrum at -69 ppm (cf. Figure II.5A). However, hydrolysis of APS in absence of acetic acid affords a less polymerized and lower cross-linked product as indicated by  $^{29}$ Si MAS NMR lines at -60 and -51 ppm indicative of  $RSiX(OSi)_2$  and  $RSiX_2(OSi)$  groups (cf. Figure II.5B) which are not fully cross-linked.

The appearance of a strong IR band near 1568 cm<sup>-1</sup> indicates the presence of NH3+ groups in the APS-imogolite Earlier studies of hydrolyzed APS on polished iron<sup>29</sup> and aluminum<sup>30</sup> mirrors and on high surface area silica gel<sup>14</sup> have resulted in the assignment of a similar band to amino groups H-bonded to surface silanols. However, analogous vibrations in aminosiloxanes have also unequivocally assigned to the formation [NH<sub>3</sub><sup>+</sup>][HCO<sub>3</sub><sup>-</sup>] groups due to reaction of the amino group with atmospheric  $CO_2$  and water.  $^{16-18}$  In our APS-imogolite reaction system the pH of the reaction mixture was adjusted to 3.6 with acetic acid. Thus, the amino group should be fully protonated during the surface coupling and surface polymerization reactions, in accord with the observed spectrum.

We attribute the increase in Si-O-Si frequency with decreasing hydrolyzed APS surface coverage to an increasing fraction of Si-O-Al bonding formed by the condensation of the siloxane to Al-OH sites on the external surfaces of the imogolite tubes. At high surface concentrations of APS most of the bound APS should resemble the pure polysiloxane in bonding and structure. Thus, the vibrational characteristics of the siloxane polymers far from the surface will be similar to those for the APS polymerized in absence of the surface. As surface coverage decreases, a greater fraction of the polymer interacts with the imogolite surface, most likely due to Si-O-Al coupling, and

the Si-O-Si frequency shifts to higher energy. We were unable to observe directly the Si-O-Al frequency which should result from the coupling of hydrolyzed APS polymer to the imagolite surface. The tubular aluminosilicate itself contains a strong, broad absorption near 940 cm<sup>-1</sup> due to Si-O-Al linkages (cf. Figure II.2C) and this absorption obscures weaker bands due to siloxane polymer coupling.

No evidence is found for the coupling of hydrolyzed APS to the intra-tubular Si-OH surfaces (cf. Figure II.1). Since the inner diameter is 8.2 Å, hydrolyzed APS in monomeric or dimeric form might be accessible to the Si-OH groups. However, initial coupling to Si-OH groups near channel openings should block the interior regions of the channel from further coupling. Furthermore, all surface-coupled APS is lost after three days of dialysis against deionized water at room temperature. If coupling to the Si-OH surface occurred, we would expect these bonds to be stable to hydrolysis, comparable in stability to other silicate surfaces functionalized by APS. 31 For these reasons it is unlikely that the interior surfaces of imogolite are silylated.

The <sup>29</sup>Si MAS NMR spectrum of the 0.5: 1.0 APS: Al reaction product (cf., Figure II.5C) indicates that the surface-bound polymer is less extensively cross-linked than the pure APS polymer prepared under analogous reaction conditions. Two resonances at -70 and -61 indicate the

fully cross-linked RSi(OSi)3 groups presence of and partially cross-linked RSiX(OSi)<sub>2</sub> groups, respectively. contrast, acid hydrolyzed APS alone contains only fully cross-linked RSi(OSi) environments. Apparently, immobilization of the polymer at the imagalite surface limits the degree of cross-linking. However. the imogolite-bound APS polymer is more extensively polymerized and cross-linked than the pure polymer formed by hydrolysis in absence of acetic acid (cf. Figure II.5B).

Although the FTIR and MAS NMR spectroscopic data are consistent with covalent coupling of a well cross-linked APS polymer to the Al-OH groups of imagolite, the surface modified products are hydrolytically unstable. Dialysis of the hydrolyzed APS-imogolite complexes results in the complete loss of polymer from the imagolite surface after three days of reaction. The hydrolysis of polymer far from the imogolite surface is expected, because the pure polymer itself also undergoes rapid hydrolysis (within hours) under However, even the APS equivalent dialysis conditions. imogolite surface is hydrolytically coupled to the unstable. No siloxane polymer, even at the sub-monolayer level, could be detected by FTIR for the products after several days of dialysis against deionized water.

Although aminosilane coupling agents are useful for the organo-functionalization of silanol mineral surfaces, they lack the desired hydrolytic stability for organofunctionalization of the curvi-linear Al-OH surfaces characteristic of imogolite. Future studies are planned which will address the question of whether the topology of the imogolite surface contributes to the hydrolytic instability of the coupled aminosiloxane bonds relative to other types of Al-OH surfaces.

LIST OF REFERENCES

#### LIST OF REFERENCES

- 1. Plueddemann, E. P. Silane Coupling Agents; Plenum: New York, 1982; Chapter 3.
- Sung, C. S. P.; Lee, S. H.; Sung, N. H. Polym. Sci. Technol. 1980, 12B, 757.
- Kulkarni, R. D.; Goddard, E. D. Int. J. Adhes. Adhes.
   1980, 1, 73.
- 4. Furukawa, T.; Eib, N. K.; Mittal, K. L.; Anderson, H. R., Jr. J. Colloid Interface Sci. 1983, 96, 322.
- 5. Alexander, J. D.; Gent, A. N.; Henriksen, P. N. J. Chem. Phys. 1985, 83, 5981.
- 6. Garbassi, E.; Occhiello, E.; Bastioli, C.; Romano, G. J. Colloid Interface Sci. 1987, 117, 258.
- 7. Mittal, K. L., Ed. Symposium on Adhesion Aspects of Polymeric Coatings; Plenum: New York, 1983.
- 8. Leary, H. J., Jr.; Campbell, D. S. Org. Coat. Appl. Polym. Sci. Proc. 1983, 46, 433.
- 9. Furukawa, T.; Eib, N. K.; Mittal, K. L.; Anderson, H. R., Jr. Surf. Interface Anal. 1982, 4, 240.
- 10. Eqashira, K.; Aomine, S. Clay Sci. 1974, 4, 231.
- 11. Leyden, D. E., Ed. Silanes, Surfaces and Interfaces; Gordon and Breach: New York, 1985.
- 12. Leyden, D. E.; Collins, W. T., Eds. Silylated Surfaces; Gordon and Breach: New York, 1978.
- 13. Farmer, V. C.; Fraser, A. R. Dev. Sedimentol. 1978, 27. 547.
- 14. Chiang, C. H.; Ishida, H.; Koenig, J. L. J. Colloid Interface Sci. 1980, 74, 396.
- 15. Colthup, N. B.; Daly, L. H.; Wiberly, S. E. Introduction to Infrared and Raman Spectroscopy; Academic: New York, 1975.

- 16. Ishida, H. In Symposium on Adhesion Aspects of Polymeric Coatings; Mittal, K. L., Ed.; Plenum: New York, 1983.
- 17. Boerio, F. J.; Williams, J. W. Proc. 36th Annu. Conf. Reinf. Plast./Compos. Inst., Soc. Plast. Ind. 1981, Section 2-F.
- 18. Naviroj, S.; Koenig, J. L.; Ishida, H. Proc. 37th Annu. Conf. Reinf. Plast./Compos. Inst., Soc. Plast. Ind. 1982, Section 2-C.
- 19. Nakamoto, K. Infrared and Raman Spectra of Inorganic and Coordination Compounds; Wiley: New York, 1986.
- 20. Cradwick, P. D. G.; Farmer, V. C.; Russell, J. D.;
   Masson, C. R.; Wada, K.; Yoshinaga, N. Nature Phys.
   Sci. 1972, 240, 187.
- 21. Barron, P. F.; Wilson, M. A.; Campbell, A. S.; Frost, R. L. Nature, 1982, 299, 616.
- 22. Goodman, B. A.; Russell, J. D.; Montez, B.; Oldfield, E.; Kirkpatrick, R. J. Phys. Chem. Minerals 1985, 12, 342.
- 23. Sudholter, E. J. R.; Huis, R.; Hays, G. R.; Alma, N. C. M. J. Colloid Interface Sci. 1985, 103, 554.
- 24. Caravajal, G. S.; Leyden, D. E.; Maciel, G. E. In Silanes, Surfaces and Interfaces; Leyden, D. E., Ed.; Gordon and Breach: New York, 1985, p. 283-303.
- 25. De Haan, J. W.; Van Den Bogaert, H. M.; Ponjee, J. J.; Van De Ven, L. J. M. J. Colloid Interface Sci. 1986, 110, 591.
- 26. Rudzinski, W. E.; Montgomery, T. L.; Frye, J. S.; Hawkins, B. L.; Maciel, G. E. J. Chromatogr. 1985, 323, 281.
- 27. Plueddemann, E. P. Proc. 24th Annu. Conf. Reinf. Plast./Compos. Inst., Soc. Plast. Ind. 1969, Section 19-A.
- 28. Plueddemann, E. P. In Analysis of Silicones; Smith, A. L., Ed.; Wiley: New York, 1974.
- 29. Boerio, F. J.; Armogan, L.; Cheng, S. Y. J. Colloid Interface Sci. 1980, 73, 416.
- 30. Boerio, F. J. Org. Coat. Plast. Chem. ACS Preprints, 1981, 44, 625.

31. Morrall, S. W., Ph.D. Thesis; Colorado State University, 1984.

#### CHAPTER III

Hydrolytic Lability of Silylated Imogolite, and Intercalation of the Silylated Tubular, Aluminosilicate in Montmorillonite.

#### A. INTRODUCTION

The modification of oxide surfaces by coupling with gamma-aminopropyltriethoxysilane (APS) and other functionalized organosilane coupling agents is finding useful applications in the areas of electrochemistry, chromatography, catalysis, and composite materials.  $^{1-6}$  In some systems, however, such as those involving  $Fe_2O_3$  and  $Al_2O_3$  surfaces, the performance characteristics of the organosilane-oxide interface is limited by the lability of the surface bonds in humid or aqueous environments.  $^{7-9}$ 

We recently have been concerned with the surface chemical properties of the novel tubular aluminosilicate imogolite. This compound has a molecularly regular outer diameter of 23 Å and an inner channel diameter of 8.7 Å. The outer surface consists of a gibbsite-like array of Al-OH groups, whereas the inner surface is composed of a regular distribution of SiOH groups. Our earlier FTIR and <sup>29</sup>Si MAS NMR studies provided evidence for the binding of APS polymer to the external alumina-like surfaces of imogolite.

Organosilane imogolite derivatives are potentially useful pillaring reagents for the synthesis of a new class of microporous tubular silicate-layered silicate (TSLS) intercalation compounds. 12 Pristine imogolite itself

functions as a pillaring reagent by intercalating into smectite clays at the monolayer level and forming regular intercalates that exhibit several orders of 001 x-ray diffraction. However, the intercalated tubes are laterally in van der Waals contact; consequently, the microporosity of the TSLS complex is restricted primarily to the internal channel of the tubes. By increasing the size of the tubes through the coupling of organo groups, one might expect to increase the lateral separation between tubes and thereby generate additional microporosity in a TSLS complex upon removing the organo groups through calcination.

The results of the present study demonstrate in part that APS-modified imogolite intercalates into Na-montmorillonite, but the resulting TSLS complex does not exhibit regular x-ray basal spacings. In an effort to better understand the surface chemistry of APS-modified imogolite, we have undertaken a study of the hydrolytic lability of this material. Also, we have included in the study the hydrolysis of APS-modified gamma-alumina in order to differentiate the hydrolytic properties of the external AlOH surface of imogolite from those of an internal SiOH surface.

#### B. EXPERIMENTAL

#### Materials

Imogolite was synthesized according to the method described by Farmer and Fraser<sup>13</sup> and purified by dialysis against deionized water. Gamma-alumina ("Catapal B") was

obtained from Vista. Na-montmorillonite (SWy-1, Source Clay Minerals Repository) was purified by sedimentation. APS was purchased from Petrarch Systems and used without further purification.

## Silylation Reactions

Silylation reactions with APS in aqueous solution were carried out using 0.17 wt. % and 0.08 wt. % suspensions of imogolite, respectively. gamma-alumina and The suspensions were adjusted to pH 4.2 with acetic acid before the addition of APS. A 2 wt. % solution of APS was adjusted to pH 4.2 with acetic acid and allowed to stir for 0.5 h. The desired amounts of APS solution were then added to the mineral suspensions, and the mixtures were allowed to stir over night. The amount of organosilane added to each suspension equaled 78 and 85 wt. % of the air-dried solid imogolite and gamma-alumina, respectively. quantities of APS used in the silylation reactions exceeded the amounts needed for monolayer coverage of the substrates. A 0.5 wt. % solution of pure APS in deionized water also was prepared, and the pH was adjusted to 3.7 with 1.0 M acetic acid.

## Hydrolysis of APS-Imogolite

The silylated alumina and imogolite suspensions were divided into 25 mL aliquots and placed into tubular cellulose dialysis membranes (Spectrapor-Spectrum Medical Industries) having a molecular weight cutoff of 12,000 to

14,000. The membrane tubes were subsequently placed into 5 L of deionized water. A membrane tube was removed every two hours for the first eighteen hours, and at longer intervals thereafter. Each time a sample was removed, the deionized water was replaced. With the exception of the hydrolyzed APS, the dialyzed suspensions were air-dried, and the amounts of bound APS were analyzed by Fourier Transform Infrared (FTIR) spectroscopy. The depletion of pristine APS polymer from the dialysis membrane was determined by allowing the solution to evaporate in air and weighing the residue recovered.

## gamma-Aminopropyltriethoxysilane-montmorillonite Complex

A 1.33 wt. % Na-montmorillonite suspension was mixed with a known volume of a 1 wt. % APS solution that had been adjusted to pH 3.7 by the addition of 1.0 M acetic acid. The mixture was allowed to dry in air to afford a composite product containing 57 wt. % APS. The product was then washed with water and air-dried.

# gamma-Aminopropyltriethoxysilane-Imogolite-Montmorillonite Complex

A 0.1 wt. % suspension of imogolite was combined with a known volume of a 1 wt. % APS solution that had been adjusted to pH 3.7 by the addition of 1.0 M acetic acid. The concentration of APS was made equal to 7 wt. % of the imogolite concentration. A volume of 1.33 wt. % Na-montmorillonite was added to the APS-treated imogolite suspensions in a weight ratio of 2.5:1

imogolite:montmorillonite. The mixture was stirred overnight, collected by centrifugation, resuspended in water and air-dried.

# Physical Measurements

X-ray diffraction patterns were obtained for oriented films formed by air-drying the suspensions on the surface of a glass slide. A Rigaku Rotaflex model RU-200BH diffractometer equipped with a copper target was used to measure basal spacings.

FTIR vibrational spectra of air-dried products were recorded over the frequency range from 4000 cm<sup>-1</sup> to 400 cm<sup>-1</sup> on an IBM model IR 40S instrument equipped with an IR44 workstation. The samples (40 mg) were weighed on an analytical balance and pressed into 2 wt. % KBr pellets. The concentration of APS in each sample was determined from the absorbance ratios of selected APS and substrate stretching frequencies. The absorbance of the  $V_{as}(NH_3)^+$  $1570 \text{ cm}^{-1} \text{ was}$ vibration at used to determine concentrations for the APS-modified imagolite and gammaalumina samples. The intensities of the silane vibrations were normalized with respect to the V(SiOAl) stretch at 954 cm<sup>-1</sup> for imagolite and the 1070 cm<sup>-1</sup> v(AlOA1) vibration in gamma-alumina. APS Concentrations for representative samples determined in this manner were confirmed by elemental concentration analysis. The data reproducible to within +/-10 percent of the reported value.

The  $^1\text{H}$  decoupled MAS  $^{29}\text{Si}$  NMR spectra were obtained on a Varian VXR400 spectrometer equipped with a Doty probe. The  $^{29}\text{Si}$  spectra were generated at a frequency of 79.459 MHz incorporating a 30 degree pulse of 3 µsec, a delay time of 20 seconds and a sample spinning rate of 5 KHz. All chemical shifts were reported with reference to TMS.

Carbon and hydrogen elemental analyses were performed by Galbraith Laboratories in Nashville, Tennessee. Silicon and aluminum elemental analysis was done at the inorganic chemistry laboratory of the Department of Toxicology at Michigan State University.

Three-point nitrogen BET surface areas for the materials were measured on a Quantachrome Quantasorb Jr. sorptometer.

#### C. RESULTS

Gamma-aminopropyltriethoxysilane (APS) is known dilute solution hydrolyze in aqueous to the organotrisilanol and an organosiloxane dimer. 7 Allowing the solution to evaporate in the open atmosphere leads to the protonation of the amino group by carbonic acid, and to condensation of APS units to form the ammoniumpropylsiloxane polymer. When an oxide surface is exposed to a hydrolyzed APS solution, the APS initially the surface hydroxyls.7 hydrogen-bonded to Dehydration normally results in the formation of a surfacecoupled organosiloxane polymer. The characterization of

the surface-bound polymer can be accomplished using FTIR and <sup>29</sup>Si MAS NMR spectroscopy.

FTIR and <sup>29</sup>Si MAS NMR measurements from previous work<sup>10</sup> have provided evidence for the formation of a surface-bound polysiloxane on imagolite upon evaporating a suspension of the substrate in 2.4 wt. % APS at pH 3.6 in air at ambient temperature. This siloxane polymer, however, was readily dissociated from the imagolite surface upon dialysis against distilled water.

In the present work we have monitored by FTIR spectroscopy the APS concentration throughout the dialysis the APS treated-imogolite suspension in order of determine the hydrolysis rate. The dialysis rate for the imogolite-bound polymer was compared with the dialysis rate for the pristine polymer under analogous conditions. expected, the diffusion of pristine polymer through the dialysis membrane was much faster than the rate of loss for the polymer coupled to imogolite. For comparison purposes, we also examined the dialysis rate for the silylated surface of gamma-alumina, an amorphous oxide having surface AlOH units. A comparison of the hydrolysis behavior could then be made for siloxane polymer bound to the bifunctional SiOH and AlOH surfaces of imagolite and the monofunctional surfaces of alumina having only AlOH sites.

The APS concentrations for the siloxane-modified imogolite and gamma-alumina samples were determined from the absorbances of selected IR bands for KBr pellets of the

air-dried samples. The concentration of pristine APS polymer was determined by weighing the residue collected from the air-dried samples after each dialysis interval.

The FTIR spectra for the starting imogolite and gamma-alumina substrates are shown in Figure III.1. Imogolite (Figure III.1A) exhibits two bands due to the presence of water, namely, the V(OH) stretching frequency near  $3500~\rm cm^{-1}$  and the  $\delta(\rm HOH)$  deformation band at  $1630~\rm cm^{-1}$ . There also are two bands at  $995~\rm cm^{-1}$  and  $940~\rm cm^{-1}$  due to V(SiOAl) stretching modes that are indicative of the isolated orthosilicate units present in the imogolite structure. The gamma-alumina FTIR spectrum, (Figure III.1B), contains prominent hydroxyl stretches in the  $3000~\rm cm^{-1}$  to  $3700~\rm cm^{-1}$  range and a sharp V(AlOAl) band, at  $1070~\rm cm^{-1}$ .

The FTIR absorbances characteristic of pristine APS polymer, formed by hydrolysis in the presence of acetic acid at pH 3.7 in aqueous acetic acid and evaporation of the solution in air at room temperature, were analyzed in detail in our previous work. Two  $V_{as}(SiOSi)$  stretching modes were assigned to absorbances at 1130 and 1030 cm<sup>-1</sup>. The  $V_{as}(CH_2)$  frequency of the propyl group and the alkylammonium ion stretching frequency,  $V_{as}(NH_3^+)$ , were assigned to bands at 2926 cm<sup>-1</sup> and 1573 cm<sup>-1</sup>, respectively. Acetic acid, along with carbonic acid formed from atmospheric  $CO_2$ , caused protonation of the amino group in the polymer. Very strong absorbances due to the

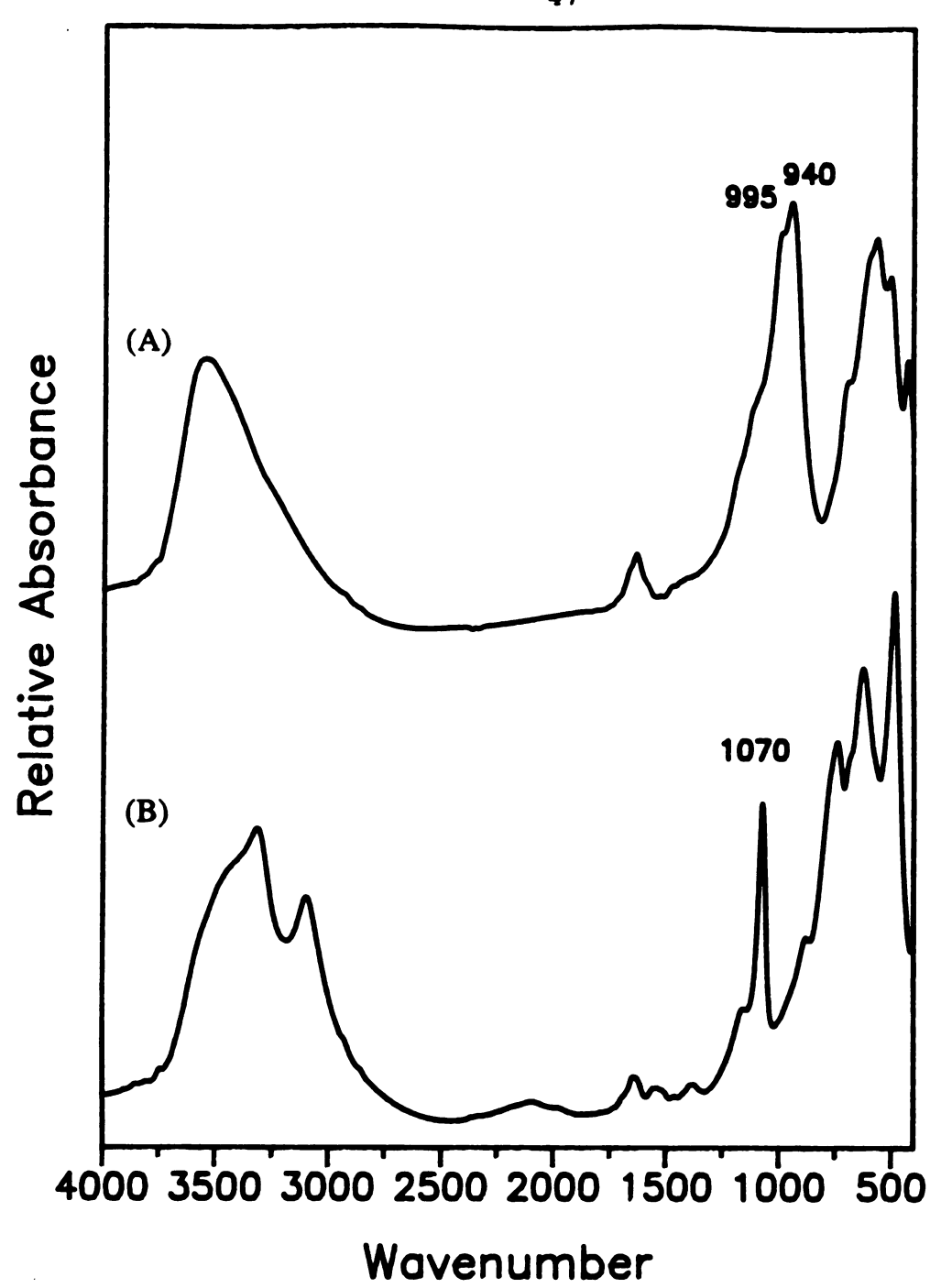


Figure III.1. FTIR absorbance spectra (KBr pellets) of the substrates (A) imagolite and (B) gamma-alumina.

counterions occurred at 1400 cm<sup>-1</sup> for the acetate  $v_s(RCO_2^-)$  stretch and at 1638 cm<sup>-1</sup> and 1336 cm<sup>-1</sup> for the bicarbonate  $v_{as}(CO_2^-)$  and  $v_s(CO_2^-)$  absorbances, respectively.

We consider next the FTIR properties of APS adsorbed on imagolite and gamma-alumina at initial loadings of 78 and 85 wt. % respectively. These loadings are in excess of the amounts necessary for monolayer coverage. On the basis of the  $N_2$  BET surface areas for imagolite (500  $m^2/g$ ) and gamma-alumina (290  $m^2/g$ ), a hydroxyl group surface concentration of  $\sim 12-14/100 \text{ Å}^2$ , and coupling of one RSiO<sub>2</sub> moiety to 3 surface OH groups, complete monolayer coverage should occur at 46 and 31 wt. % APS, respectively. course, these values represent upper loading limits for ideal monolayer coverage because they are based estimates that disregard the surface occupied by the organo groups and the formation of siloxane polymer. Vibrational frequencies due to the polysiloxane were readily observed in the FTIR spectra of the initial APS-modified samples. Spectra obtained after dialysis periods of 0, 4, 12 and 50 hours are shown for the APS-modified imagolite and gammaalumina systems in Figures III.2 and III.3, respectively.

The siloxane was identified in the spectra of the initial samples by a band in the 1120 to 1140 cm<sup>-1</sup> region which was assigned to the asymmetric stretching frequency of SiOSi linkages in the polymer. <sup>16</sup> An alkylammonium ion stretching frequency,  $v_{as}(NH_3^+)$ , similar to that observed in the pure polymer, was found near 1570 cm<sup>-1</sup>. The acetic

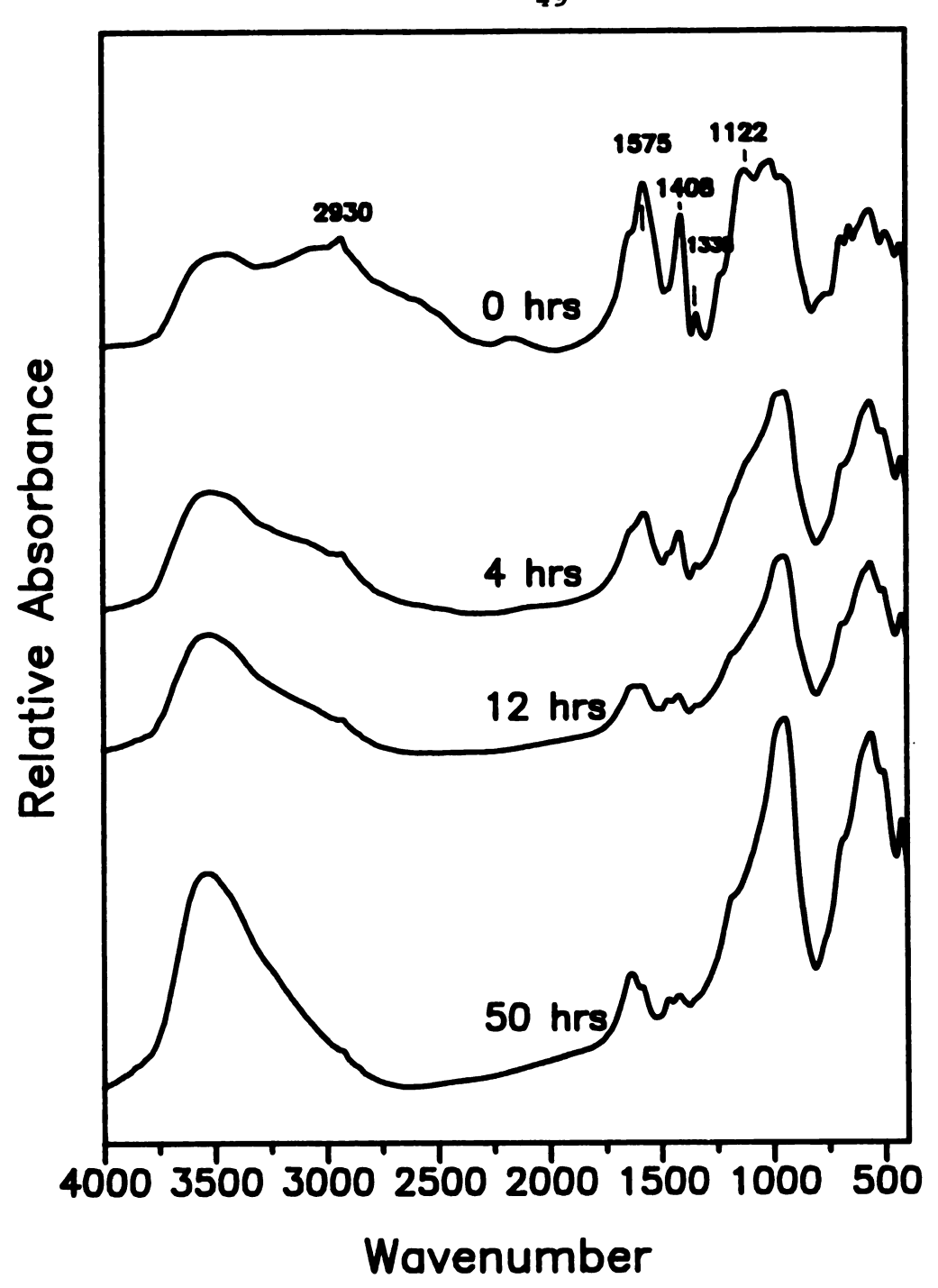


Figure III.2. FTIR absorbance spectra (KBr pellets) of APS-modified imagolite samples isolated after dialysis for the time intervals indicated.

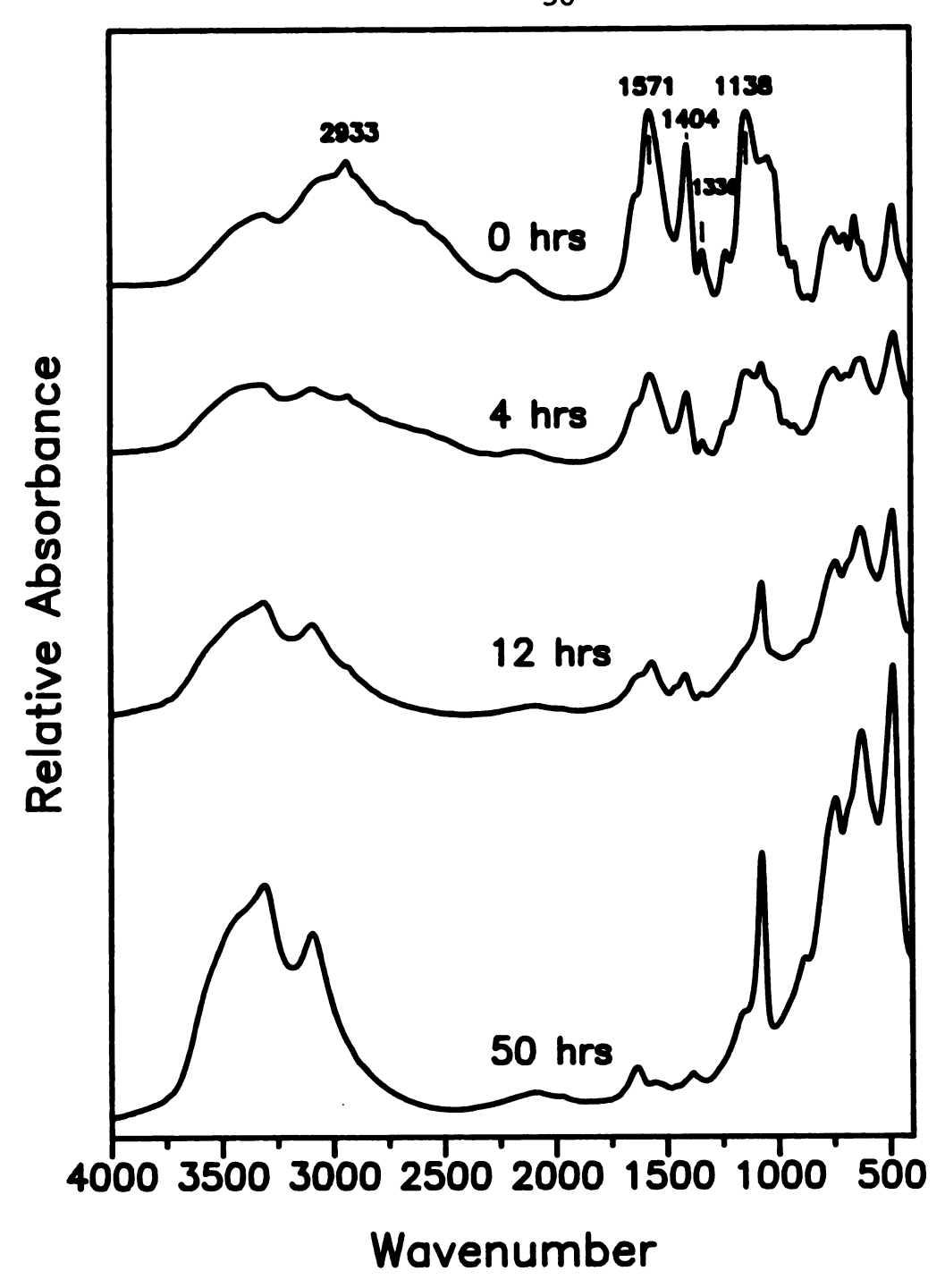


Figure III.3. FTIR absorbance spectra (KBr pellets) of APS-modified gamma-alumina samples isolated after dialysis for the time intervals indicated.

acid responsible for the initial protonation of the amine, gives rise to the strong acetate  $V_{\rm S}({\rm RCO_2}^-)$  band near 1400 cm<sup>-1</sup>. The amine also reacts with carbonic acid formed by atmospheric CO<sub>2</sub>. Vibrations due to the presence of bicarbonate ion were visible at 1638 cm<sup>-1</sup> due to  $V_{\rm as}({\rm CO_2}^-)$ , and 1336 cm<sup>-1</sup> due to  $V_{\rm s}({\rm CO_2}^-)$ . The sharp band near 2930 cm<sup>-1</sup> has been assigned to the  $V_{\rm as}({\rm CH_2})$  frequency of the propyl group.

As dialysis time was increased, a sharp reduction in siloxane absorbances relative to the substrate absorbances was observed for each of the APS-modified substrates. A comparison of the FTIR spectra for the pristine substrates in Figure III.1, with the APS-modified substrates Figures III.2 and III.3, provides verification for the retention of significant amounts of siloxane polymer by both substrates after 12 hours of dialysis. The presence of the gamma-aminopropyl group is especially visible in the  $V_{as}(CH_2)$  stretching region near 2930 cm<sup>-1</sup> and in the alkylammonium ion stretching frequency,  $V_{as}(NH_3^+)$ , near 1570 cm<sup>-1</sup>. The latter absorbance was utilized in the determination of the siloxane concentration. After twelve hours of dialysis, the APS concentration was 40 and 24 wt. % for the imogolite and gamma-alumina substrates, respectively. These values begin to approach the values expected for ideal monolayer coverage for the two substrates.

Plots of the log [wt. % APS] versus dialysis time for the pristine APS, APS-modified imagolite and APS-modified gamma-alumina systems are shown in Figure III.4. Although these data are not suitable for detailed kinetic treatment. the relative APS labilities can be expressed empirically by the time required to hydrolytically remove half of the polymer  $(t_{1/2})$ . For pristine APS, the  $t_{1/2}$  value estimated from the Figure is only 1.7 hours. The monomeric and dimeric units that form upon APS hydrolysis are depleted rapidly through the pores of the dialysis membrane. particularly significant that the depletion of the pristine APS from the dialysis membrane is at least five times as as the depletion of polymer from APS-modified imogolite and gamma-alumina. Thus, the polymer depletion in these latter cases is limited by the hydrolytic displacement of the polymer from the substrate surfaces.

Bimodal depletion behavior was observed for the dialysis of both APS-modified imagolite and gamma-alumina. At the initial stages of dialysis where the APS surface concentration is in excess of a monolayer, the depletion rates were similar  $(t_{1/2} = 10 \text{ h})$ . However, at longer dialysis times the depletion rate decreased for the APS-modified imagolite and gamma-alumina. At polymer loading below monolayer levels, <46 wt. % for imagolite, the depletion of polymer from APS-modified imagolite slowed to  $t_{1/2} = 63 \text{ h}$ , whereas the depletion rate for the APS-modified gamma-alumina increased to  $t_{1/2} = 2.4 \text{ h}$ .

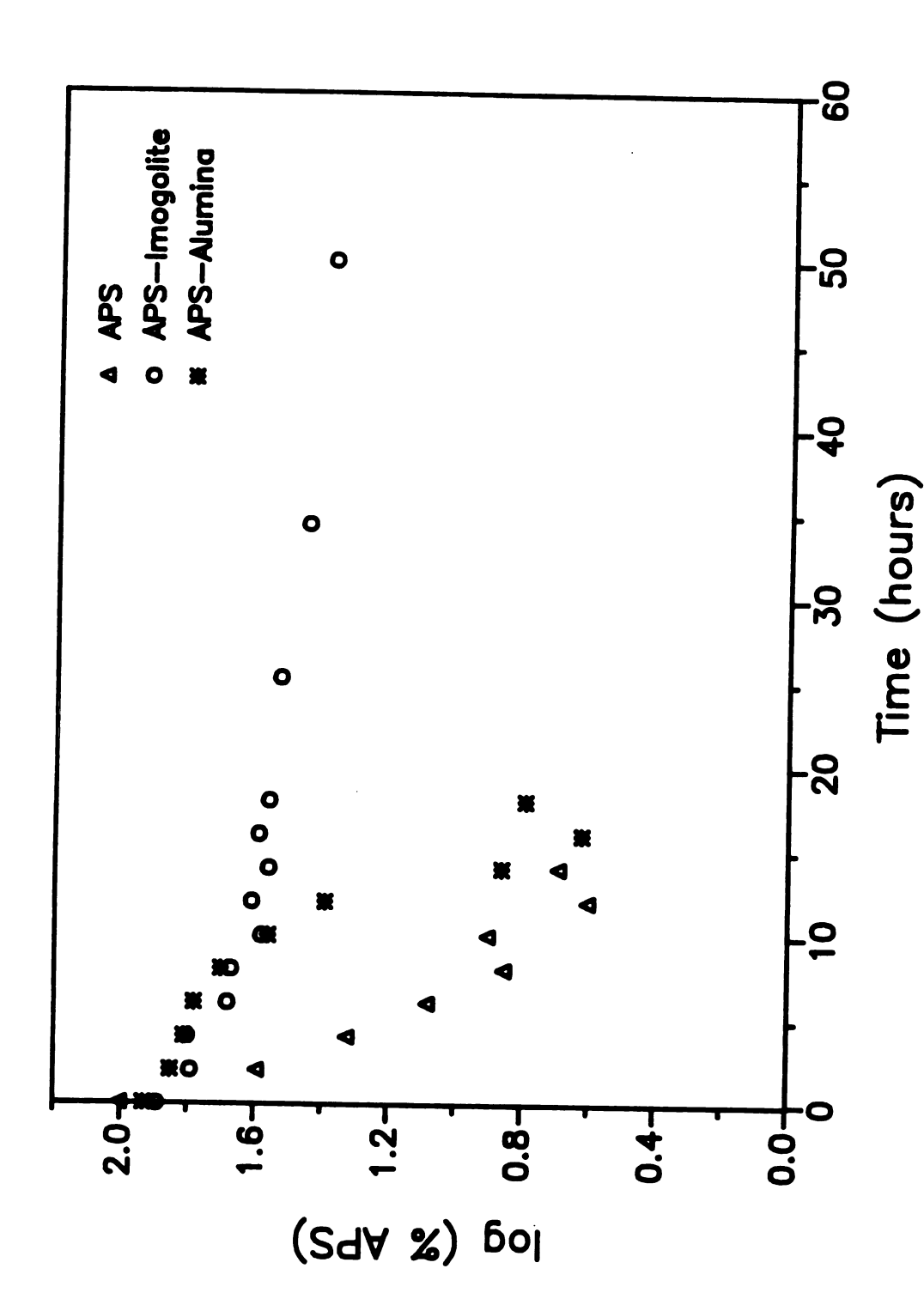


Figure III.4. Plot of log(wt. % APS) versus dialysis time for the hydrolyzed APS polymer, APS-modified imogolite and APS-modified gamma-alumina.

In an effort to characterize the polymer adsorbed on imogolite and gamma-alumina, the modified oxides investigated by <sup>29</sup>Si MAS NMR. The spectrum for APSmodified imagolite at a 20 wt. % concentration is shown in Figure III.5A. This sample was prepared by direct reaction with APS at pH 3.7, and did not undergo dialysis. However, dialyzed samples showed the same characteristic NMR spectra as non-dialyzed samples at comparable APS loading. spectrum contains a very intense resonance at -79 ppm due to the HOSi(OAl)3 environment of the unmodified imagolite orthosilicate units. 17,18 The envelope of resonances in the -45 ppm to -70 ppm region contains a shoulder at -48 ppm and two resolved resonances at -58 ppm and -68 ppm. These three resonances were assigned to the following silicon sites of the surface bound polymer: RSi(OH)2(OM),  $RSi(OH)(OM)_2$  and  $RSi(OM)_3$  where M is an adjacent Si site in the polymer, or an Al or Si site at the imagolite surface. These assignments are in accord with the chemical shifts observed for APS-modified silica surfaces. 19-23 broad resonance at -90 ppm is assigned to silylated silicon sites in the imogolite structure. The 11 ppm shift upfield is consistent with the conversion of some imagolite Si(OH)(OAl) sites at the inner surface of the tubes to Si(OSi)(OAl)<sub>3</sub> sites by reaction with APS.

The <sup>1</sup>H decoupled <sup>29</sup>Si MAS NMR spectrum of APS modified gamma-alumina at a 24 wt. % concentration is shown in Figure III.5B. This sample also was prepared by the direct



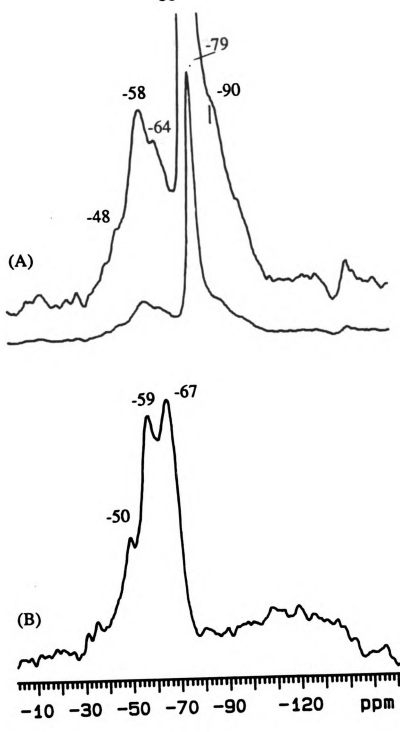


Figure III.5.  $^1\text{H}$  decoupled  $^{29}\text{Si}$  MAS NMR (79.459 MHz) spectra of (A) 20 wt. % APS-modified imagolite and (B) 24 wt. % APS-modified gamma-alumina samples using a 3 us pulse width, a relaxation delay time of 20 s, and a sample spinning rate of 5 kHz.

reaction with APS at pH 3.7 without undergoing dialysis. Resonances due to the surface-coupled polymer at -50 ppm, -59 ppm and -67 ppm were assigned to  $RSi(OH)_2(OM)$ ,  $RSi(OH)(OM)_2$  and  $RSi(OM)_3$  (M = Si, Al) sites, respectively. Here, the lines are sharper than the corresponding lines for APS-modified imagolite. The reduced linewidth suggests that the APS siting is less heterogeneous on the monofunctional alumina surface.

Table III.I summarizes the <sup>29</sup>Si MAS NMR chemical shift assignments for APS-modified imogolite and gamma-alumina. Included in the table are the shifts for pristine polymer prepared at pH 3.7 and at the ambient pH value of 10. The values for the oxide bound polymer are shifted slightly downfield from those observed for the pristine polymer. It is noteworthy that the extent of APS crosslinking on the metal oxide surfaces at pH 3.7 is less than that observed for pristine polymer prepared at the same pH. In fact, the distribution of the organosilicon sites on the imogolite and gamma-alumina surfaces are similar to those observed for APS polymerized at ambient pH 10.

We next investigated whether APS-modified imogolite could be intercalated into the galleries of a Namontmorillonite clay to form a tubular silicate layered silicate (TSLS) intercalation complex. The APS-modified imogolite intercalation in Na-montmorillonite was anticipated because the positive charge provided by the APS polymer should allow for electrostatic interaction between

Table III.I. 29Si chemical shifts for silicon environments in pristine APS polymer, APS-modified Imogolite and APS-modified γ-Alumina.

SAMPLE	RSi(OH) <sub>2</sub> (OM)*	RSi(OH) <sub>2</sub> (OM)* RSi(OH)(OM) <sub>2</sub>	RSi(OM) <sub>3</sub>	Si(OH)(OAl)3	Si(OSi)
APS-modified Imogolite <sup>b</sup>	- 48	-58	1	-79	06-
APS-modified y-Alumina <sup>b</sup>	-50	-59	89-	ı	
APS polymerized at pH 3.5	•	•	69-	•	•
APS polymerized at pH 10	-51	09-	69-	1	•

<sup>a</sup> M = Si or Al. <sup>b</sup> These samples were prepared at pH 3.5

the negatively charged clay layers. However, hydrolyzed APS itself may compete with APS-modified imagolite for intercalation in montmorillonite. Therefore, prior to investigating the reaction of APS-modified imagalite with Na-montmorillonite, we examined the reaction of the clay with hydrolyzed APS at pH 3.7. Figures III.6A and III.6B the diffraction compare x-ray patterns for Namontmorillonite before and after treatment with sufficient hydrolyzed APS solution to give a 57 wt. concentration at pH 3.9. A highly ordered single phase was obtained with a 21.3 Å d<sub>0.01</sub> spacing, as compared with a 12.7 Å spacing for the air-dried Na-montmorillonite. Upon washing the product with deionized water, the d-spacing for the air-dried product decreased to 18 A and finally to 14.4 Å as shown by the x-ray patterns in Figures III.6C and III.6D.

Figure III.7 shows the x-ray diffraction pattern of the air-dried product obtained by the reaction of a 7 wt. % APS-modified imogolite suspension with a Na-montmorillonite suspension at a weight ratio of 2.5:1 imogolite:clay. Also, included are the x-ray diffraction pattern of the product after one and two washings with water. The unwashed product exhibits very diffuse reflections near 15 and 34 Å. Washing the product with water improves the crystallographic ordering and leads to an imogolite-intercalated montmorillonite with a 35.6 Å d<sub>001</sub> spacing. This spacing is identical to the value obtained for TSLS

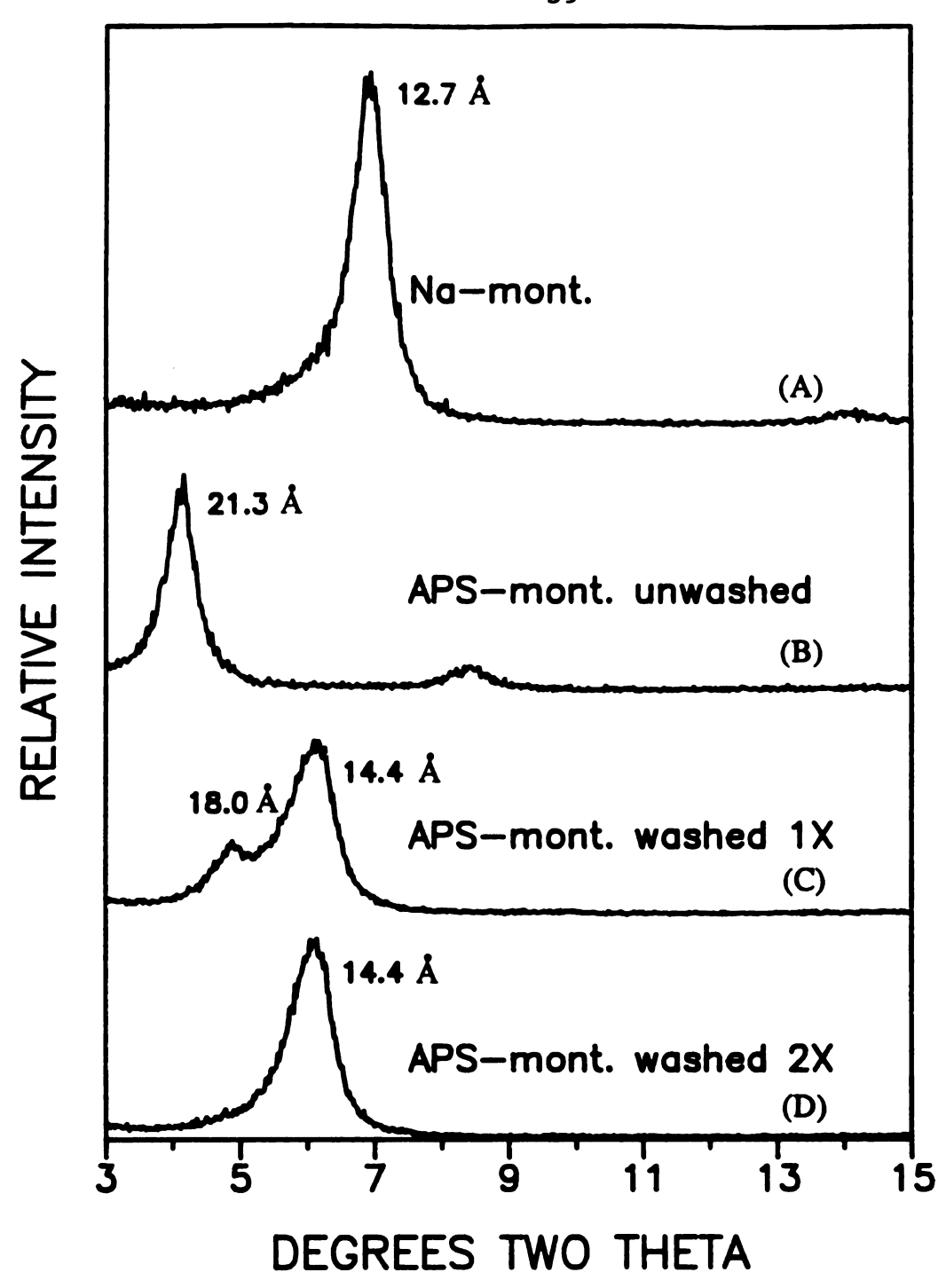


Figure III.6. X-ray diffraction patterns of oriented films of (A) Na-montmorillonite, (B) 57 wt. % APS-modified Na-montmorillonite, (C) sample in (B) washed once with  $\rm H_2O$ , and (D) sample in (B) washed twice with  $\rm H_2O$ .

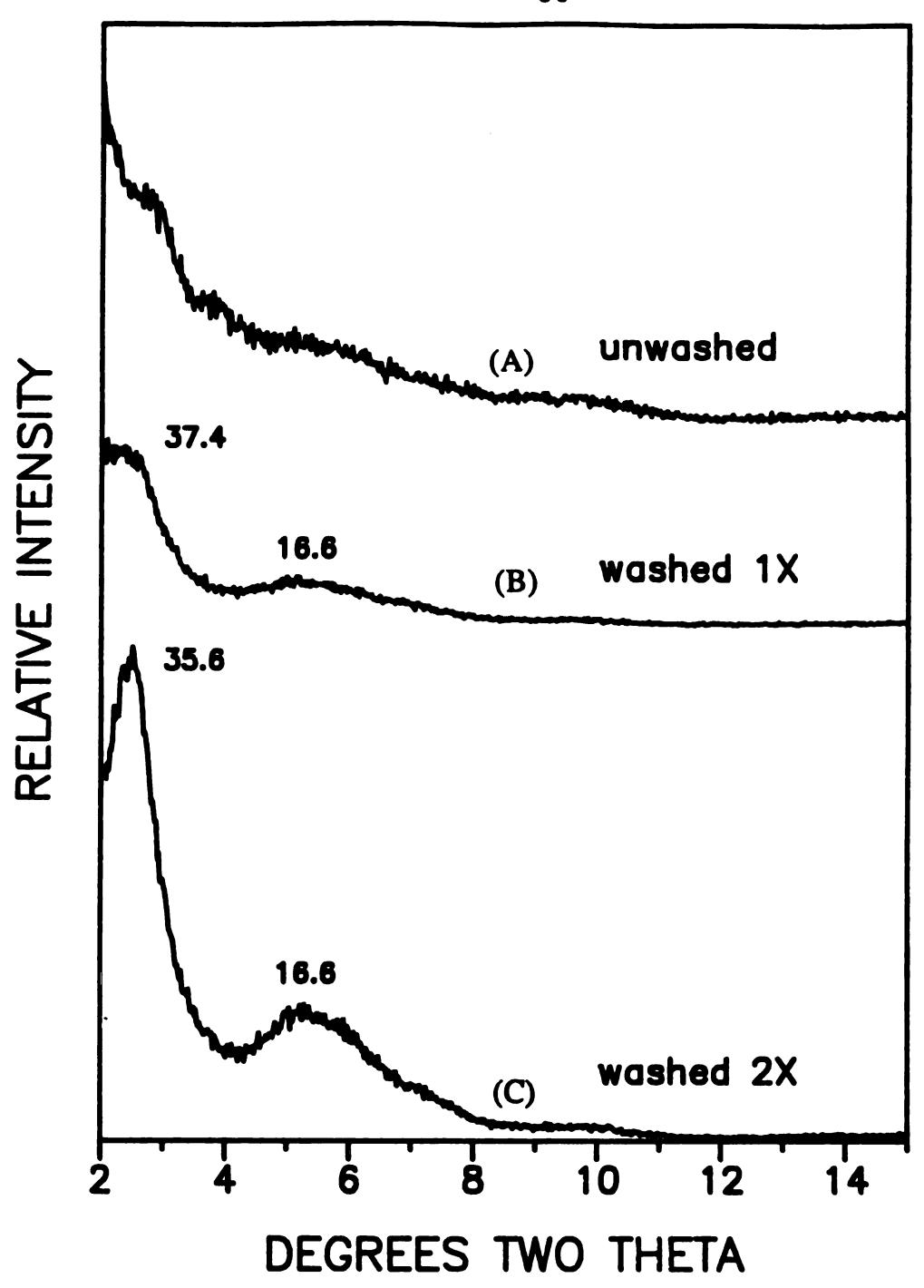


Figure III.7. X-ray diffraction patterns of oriented films of (A) 7 wt. % APS-modified imogolite suspension combined with a Na-montmorillonite suspension in a wt. ratio of 2.5:1 imogolite to clay, (B) sample in (A) washed once with water and (C) sample in (A) washed twice with water.

formed by intercalation of pristine imagolite into Namontmorillonite. 11 Clearly, the TSLS reaction products are easily distinguishable by x-ray diffraction from APS-intercalated montmorillonite.

TSLS products were also obtained using APS-modified imogolite at concentrations of 15 and 30 wt. %. These TSLS products behaved similarly to the material obtained using 7 wt. % APS. The unwashed products exhibited highly diffuse x-ray patterns. Subsequent washings yielded products with x-ray diffraction patterns characteristic of ordered systems having basal spacings of 35 to 37 Å, typical of pristine imogolite intercalated montmorillonite products.

### D. DISCUSSION

Within experimental uncertainty, identical depletion rates  $(t_{1/2}=10 \text{ hr})$  were observed for APS-modified imagolite and APS-modified gamma-alumina at loadings corresponding to multilayer APS coverage. This result suggests that the structure of the APS polymer far from the substrate surface is similar in both systems. However, substrate dependent depletion rates were observed for polymer loadings below approximately 48 wt. % APS. The half-life for APS depletion from APS-modified imogolite decreased dramatically ( $t_{1/2} = 63$  hours) at low APS loadings compared with that observed for higher loadings. On the other hand, the rate of APS removal from APS-modified gamma-alumina increased  $(t_{1/2} = 2.4 \text{ hours})$  at low APS loadings (cf.

Figure III.4). These differences in depletion rates at low APS loadings suggest that the APS binding mechanism depends on the nature of the substrate.

The nature of the APS polymer-surface coupling was probed by <sup>1</sup>H decoupled <sup>29</sup>Si MAS NMR. <sup>1</sup>H decoupled <sup>29</sup>Si MAS NMR results from an APS-modified gamma-alumina sample having an APS loading of 24 wt. %, cf. Figure III.5B, showed the presence of RSi(OH)2(OM), RSi(OH)(OM)2, and  $RSi(OM)_3$  resonances, where M = Si, Al linkages. Resonances having chemical shifts and relative intensities of pristine APS polymerized at ambient pH dominate the spectrum. Therefore, few covalent polymer linkages to the gammaalumina surface exist at submonolayer APS loadings on APSmodified gamma-alumina. The effects of isolated covalent or non-covalent polymer-surface coupling are indirectly demonstrated by the extent of crosslinking observed. the presence of gamma-alumina at pH 3.5, APS polymerizes to a moderately crosslinked form characteristic of pristine APS polymerized at pH 10. Under conditions of reduced pH, in the absence of gamma-alumina, pristine APS polymerizes to a fully crosslinked form, characterized by the presence of a single RSi(OSi), resonance. These results do not allow the identification of the binding mechanism, but together with the hydrolysis behavior, they suggest that polymer crosslinking is inhibited by the isolation of APS units immobilized on the alumina surface.

 $^{29}$ Si MAS NMR was used to explain the reduced polymer depletion rate for APS-modified imagolite samples at low APS loading. The <sup>1</sup>H decoupled <sup>29</sup>Si MAS NMR spectrum of a 20 wt. % APS-modified imagolite sample, cf. Figure III.5A. exhibits resonances due to  $RSi(OH)_{3-x}(OM)_{x}$ M = Si, Al. In contrast to the APS-modified gamma-alumina spectrum, the chemical shifts and relative intensities of resonances observed were unique to the APS-modified imogolite, suggesting a large percentage of polymer-surface linkages. The chemical shifts of the resonances in this spectrum were shifted downfield from typical pristine polymer resonances. The intensity of the RSi(OH)(OM)<sub>2</sub> resonance was enhanced, compared with the other polymer resonances in the APS-modified material. A resonance due to polymer coupled to imagolite silicon sites (-90 ppm) of the form (AlO)3(SiO)RSi(OM)2 gave direct evidence for covalent binding of the polymer to the internal SiOH surfaces of imogolite. The channel, 8.7 Å in diameter, accessible to hydrolyzed APS units from the ends of the tubes, is depicted in a schematic representation of a cross section of the imogolite structure in Figure III.8. Deconvolution analysis of the resonances in the 20 wt. % APS-modified imagolite <sup>29</sup>Si MAS NMR spectrum from Figure III.5A, indicate that 36 percent of the imogolite silicon sites were coupled to APS. The mole ratio of APS silicon sites to coupled imagolite silicon sites was found to be approximately equal to 1, indicating that SiOH surface

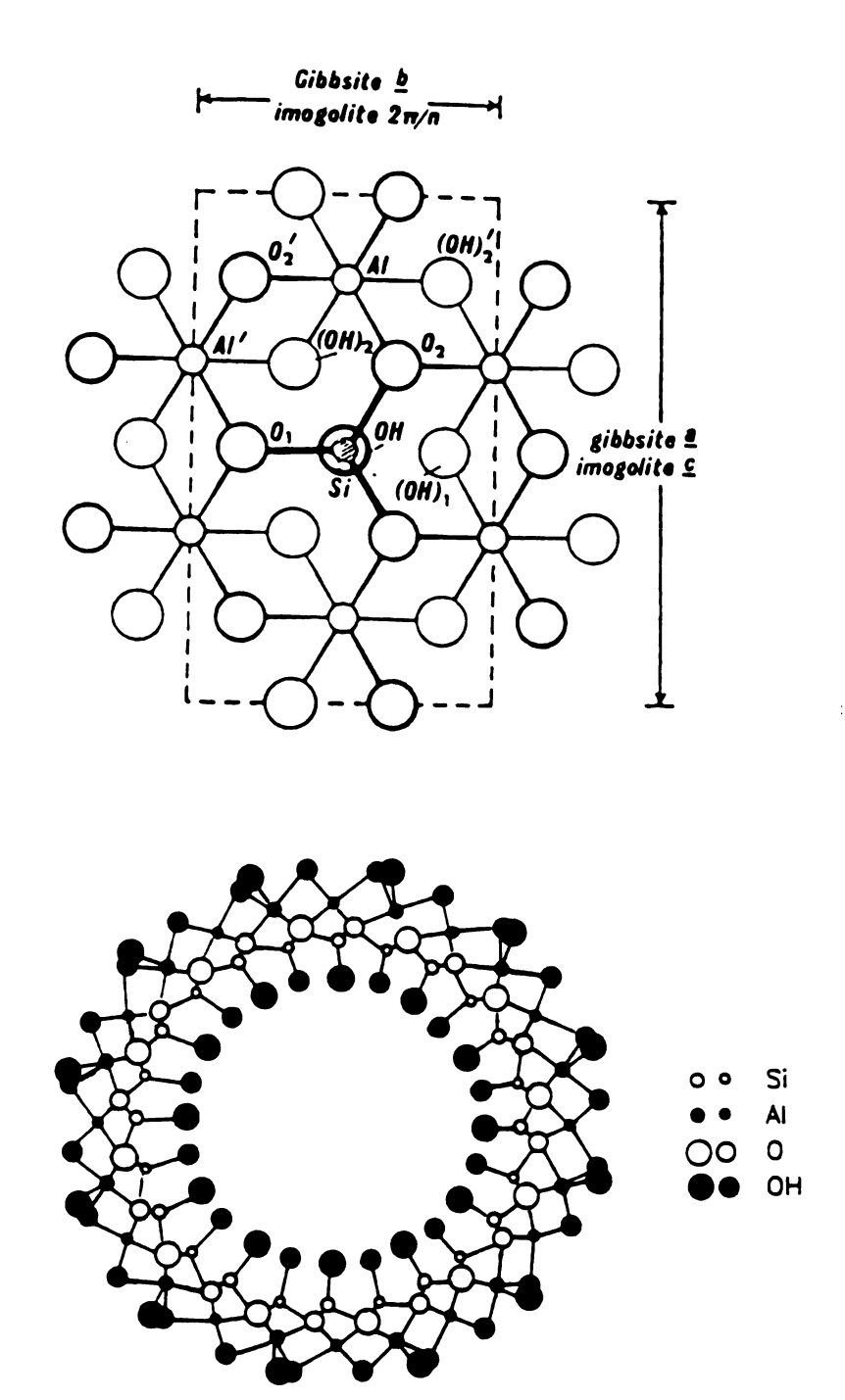


Figure III.8. Schematic representation of a cross sectional view of the imogolite structure. The tube walls are composed of five tiers of atoms. Reading from the inner to the outer wall, the tier compositions are HO, Si, O, Al, and OH, respectively. The diameter of the channel, 8.7 Å, is sufficiently large to accommodate APS as a silylating agent.

coupling is favored over AlOH surface coupling at this polymer loading. Both the NMR and the hydrolysis data show that at low polymer loading, APS polymer is covalently bonded to SiOH sites within the imagolite channel in APS-modified imagolite.

reaction of The Na-montmorillonite in aqueous suspension with APS-modified imagolite at pH 3.7 yielded a TSLS product with a very diffuse x-ray pattern. Air-dried Na-montmorillonite normally exhibits a pattern with several rational orders of 001 reflections corresponding to a basal spacing of 12.7 Å. Therefore, the diffuse pattern observed for the APS-modified TSLS complex is indicative of the formation of an interstratified intercalate. Washing the interstratified product with water results in the loss of some APS and the formation of ordered TSLS products having a 35 Å basal spacing. This basal spacing corresponds to the sum of the van der Waals thickness of the clay layer (10 Å) and the hydrated imagolite tubes (25 Å). Although APS remains bonded to the imagolite tubes, as evidenced by characteristic vibrations at 2926 cm<sup>-1</sup> and 1570 cm<sup>-1</sup>, the presence of a 35 Å basal spacing for the APS-modified imogolite/clay intercalate precludes the possibility of APS binding to the external AlOH surface of the tubes. result provides further evidence for the binding of APS in the internal channel of imogolite at low APS loadings.

The lability of APS at the external AlOH surfaces of imogolite complicates the use of APS-modified imogolite as

a precursor to microporous TSLS derivatives. Thus far we have been unable to utilize the functionalized tubes as a means of uniformly spacing the tubes as pillars in the galleries of smectite clay. A more viable approach currently being investigated, involves the use of organophosphates or organophosphonic acids coupling agents modification of the external AlOH surfaces for imogolite. The results obtained from these latter studies will be reported elsewhere.

LIST OF REFERENCES

### LIST OF REFERENCES

- Moses, P.R.; Wier, L.M.; Lennox, J.C.; Finklea, H.O.; Murray, R.W. Analyt. Chem. 1978, 50, 576.
- Silylated Surfaces; Leyden, D.E.; Collins, W.T., Eds.;
   Gordon and Breach: New York, 1980.
- 3. Silanes, Surfaces and Interfaces; Leyden, D.E., Ed.; Gordon and Breach: New York, 1985.
- 4. Chemically Modified Oxide Surfaces; Leyden, D.E.; Collins, W.T.; Lochmuller, C.H., Eds.; Gordon and Breach: New York, 1990.
- 5. Sung, C.S.P.; Lee, S.H.; Sung, N.H. Polym. Sci. Technol. 1980, 12B, 757.
- 6. Garbassi, F.; Occhiello, E.; Bastioli, C.; Romano, G.; J. Colloid Interface Sci. 1987, 117, 258.
- 7. Plueddemann, E.P. Silane Coupling Agents; Plenum: New York, 1982.
- 8. Kulkarni, R.D.; Goddard, E.D. Int. J. Adhes. Adhes. 1980, 1, 73.
- 9. Furukawa, T.; Eib, N.K.; Mittal, K.L.; Anderson, H.R., Jr. J. Colloid Interface Sci. 1983, 96, 322.
- 10. Johnson, L.M.; Pinnavaia, T.J. Langmuir 1990, 6, 307.
- 11. Cradwick, P.D.G.; Farmer, V.C.; Russell, J.D.; Masson, C.R.; Wada, K.; Yoshinaga, N. Nature Phys. Sci. 1972, 240, 187.
- 12. Johnson, I.D.; Werpy, T.A.; Pinnavaia, T.J. J. Am. Chem. Soc. 1988, 110, 8545.
- 13. Farmer, V.C.; Fraser, A.R. Dev. Sedimentol. 1978, 27, 547.
- 14. Maciver, D.S.; Tobin, H.H.; Barth, R.T. J. Catalysis 1963, 2, 485.

- 15. Caravajal, G.S.; Leyden, D.E.; Maciel, G.E. In Silanes Surfaces and Interfaces; Leyden, D.E., Ed.; Gordon and Breach: New York, 1985; pp 283-303.
- 16. Sudhoter, E.J.R.; Huis, R.; Hays, G.R.; Alma, N.C.M. J. Colloid Interface Sci. 1985, 103, 554.
- 17. Barron, P.F.; Wilson, M.A.; Campbell, A.S.; Frost, R.L. Nature 1982, 299, 616.
- 18. Goodman, B.A.; Russell, J.D.; Montez, B.; Oldfield, E.; Kirkpatrick, R. J. Phys. Chem. Miner. 1985, 12, 342.
- 19. Cradwick, P.D.G.; Farmer, V.C.; Russell, J.D.; Masson, C.R.; Wada, K.; Yoshinaga, N. Nature Phys. Sci. 1972, 240, 187.
- 20. Chiang, C.H.; Ishida, H.; Koenig, J.L. J. Colloid Interface Sci. 1980, 74, 396.
- 21. Engelhardt, G.; Michel, D. High-Resolution Solid-State NMR of Silicates and Zeolites; Wiley: New York, 1987; p 211.
- 22. De Haan, J.W.; Van Den Ven, L.J.M. J. Colloid Interface Sci. 1986, 110, 591.
- 23. Rudzinski, W.E.; Montgomery, T.L.; Frye, J.S.; Hawkins, B.L.; Maciel, G.E. J. Chromatogr. 1985, 323, 281.

### CHAPTER IV

Reaction of Gamma-aminopropylphosphonic Acid with Imogolite and Na-montmorillonite

### A. INTRODUCTION

Imogolite is a tubular aluminosilicate with molecularly regular outer diameter of 23 Å, an internal channel diameter of 8.7 Å and a length of 2000 to 3000 Å.1 We have recently shown that the tubular structure can be directly intercalated as a regular monolayer into the galleries of smectite clays to form a new class of clavs.<sup>2</sup> microporous pillared Nitrogen adsorption measurements and selective adsorption studies showed that the microporosity of the material originated primarily from the void volume provided by the imagolite intra-tube channel.<sup>3</sup> Relatively little void volume was provided between the tubes due to their tendency to cluster in van der Waals contact. The imogolite intercalated montmorillonite complex was denoted tubular silicatelayered silicate or TSLS. TSLS H-bonding interactions, and the close packing of the imagolite tubes resulted in thermal stability enhancement of the intercalated tubes (>400°C) relative to pure imagolite (350°C).

More recently, we have become interested in modifying the external surfaces of imogolite as a means for the rational design of new TSLS complexes. Specifically, the intercalation of a uniformly surface-modified imogolite pillar into the galleries of Na-montmorillonite was thought to introduce lateral separation between the tubes, thereby

increasing the microporosity of the complex. Our first attempts at the surface modification of imogolite utilized organosilane coupling agents which readily form covalent bonds with hydroxylated surfaces. 4 The results of the coupling reaction between hydrolyzed the hydroxylated aminopropyltriethoxysilane (APS) and imogolite have been reported elsewhere.<sup>5</sup> surfaces of Hydrolyzable aminoalkylsilanes were attractive reagents due to their ability to afford monomeric trisilanols having protonated amino groups from acidic solutions. protonated amino groups ensure that the APS-modified imogolite retains the net positive charge necessary for subsequent intercalation reactions. The coupling between APS and the AlOH sites on the external surfaces of imogolite was found to be too labile to allow the formation of an ordered, APS-modified TSLS complex.

In the present work, we investigated the surface reaction chemistry of imogolite and gammaaminopropylphosphonic acid. Effective coupling has been demonstrated between phosphorus acids and alumina surfaces. 6-9 The aminoalkylphosphonic acids, like the aminoalkylsilanes, possess protonatable amino groups to allow the coupled imogolite surface to retain a net positive charge. The products obtained by the reaction of gamma-aminopropylphosphonic acid with Na-montmorillonite were characterized in addition to the products of the reaction between gamma-aminopropylphosphonic acid-modified imagolite and Na-montmorillonite.

### B. EXPERIMENTAL

Imogolite was synthesized according to the method described by Farmer and Fraser<sup>10</sup> and purified by dialysis against deionized water. The gamma-aminopropylphosphonic acid was purchased from Sigma and used without further purification. Na-montmorillonite, (SWy-1, Source Clay Minerals Repository) with a cation exchange capacity of 88 meg/100 g, was purified by sedimentation.

# Reactions of gamma-aminopropylphosphonic acid with Namontmorillonite

An 18 mM solution of APP in deionized water was prepared at an ambient pH of 3.9. A portion of a 1.33 wt. % aqueous Na-montmorillonite suspension was added to enough APP solution to achieve a 1:1 (w/w) ratio of clay: APP, corresponding to 5.9 moles APP per equivalent of The final pH of the suspension was 5.3. After a clav. reaction time of 16 hours, the suspension was poured onto a large glass plate and allowed to evaporate in air at room temperature. The unwashed reaction products were recovered from the plate. A second reaction of APP with Nacarried under identical montmorillonite out was stoichiometric conditions, but the pH of the 18 mM APP solution was adjusted to 7.5 with 1 M NaOH. After a reaction time of 16 hours, the suspension was allowed to air dry and the unwashed product was recovered.

Reactions of gamma-aminopropylphosphonic acid with imagolite

A 0.1 wt. % suspension of imagolite was combined with amount of solid APP sufficient an to achieve an APP: imagained weight ratio of 0.43:1, corresponding to 1 mole of APP per mole of aluminum. Half of the resulting suspension at pH 5.3 was adjusted to pH 2.6 with 1M HCl. The remaining portion was adjusted to pH 7.5 with 1M NaOH. The suspensions were allowed to stir overnight, poured onto glass plates and air-dried at room temperature.

# Reactions of gamma-aminopropylphosphonic acid treated imagolite with Na-montmorillonite

A volume of 1.33 wt. % Na-montmorillonite suspension was added to a suspension of APP treated imagolite, as prepared above at pH 7.5, to obtain a weight ratio of 2.5:1 imagolite to montmorillonite. The mixture was stirred overnight. The reaction products were then separated from the supernatent by centrifugation, resuspended in deionized water and air-dried.

### Physical Measurements

FTIR spectra of solid samples prepared as 2 wt. % KBr pellets were taken over the frequency range from 4000 cm<sup>-1</sup> to 400 cm<sup>-1</sup> on a Nicolet model IR42 spectrometer with a resolution of 4 cm<sup>-1</sup>. Difference spectra were obtained by weighted digital subtraction of absorbance spectra over the entire frequency range. Baseline corrections were not needed.

The <sup>1</sup>H decoupled <sup>31</sup>P MAS NMR and <sup>29</sup>Si MAS NMR spectra were obtained on a Varian VXR 400 spectrometer equipped with a Doty probe. The <sup>31</sup>P spectra were generated at a frequency of 161.903 MHz with a 90 degree pulse of 4.8 microseconds, and a relaxation delay time of 60 seconds at sample spinning rates of 2 to 4 kHz. Chemical shifts were reported with reference to 85% H<sub>3</sub>PO<sub>4</sub>. The <sup>29</sup>Si spectra were generated at a frequency of 79.459 MHz with a 90 degree pulse of 6.7 microseconds and a relaxation delay time of 120 seconds. Chemical shifts were reported with respect to TMS.

X-ray diffraction patterns were obtained from oriented films of the suspensions air-dried on the surface of a glass slide. A Rigaku Rotaflex model RU-200BH diffractometer equipped with a copper target (Cu  $K_{\alpha}$  radiation) and the Rigaku D/Max powder diffraction system was used to measure basal spacings.

Elemental analyses were performed by Galbraith Laboratories in Nashville, Tennessee.

Three-point nitrogen BET surface areas were measured on a Quantachrome Quantasorb Jr. sorptometer.

### C. RESULTS AND DISCUSSION

### Gamma-aminopropylphosphonic acid (APP)

Gamma-aminopropylphosphonic acid (APP) is known from x-ray crystallographic analysis  $^{11}$  to adopt a neutral zwitterionic structure,  $^{+}NH_{3}(CH_{2})_{3}PO_{3}H^{-}$ , in the solid

state. In solution, four species at different levels of protonation can be obtained. The stepwise acid dissociation constants for the three protonated species reported by Appleton et al.<sup>12</sup> are listed in Table IV.I. A reference to the abbreviations adopted for the identification of these species is also included in Table IV.I. The species of interest are identified by the letters APP followed by the net charge on the molecule. For example, +NH<sub>3</sub>(CH<sub>2</sub>)<sub>3</sub>PO<sub>3</sub>H<sub>2</sub> is denoted APP<sup>+</sup>, and +NH<sub>3</sub>(CH<sub>2</sub>)<sub>3</sub>PO<sub>3</sub><sup>2-</sup> is designated APP<sup>-</sup>.

The characterization of the APP treated materials was approached in this manner. First, the equilibrium solution APP species and the APP species isolated as reaction products were identified. Next, the APP reactant and product species were compared. Finally, a description of the chemical interactions between the APP and mineral reactants which might be responsible for the observed differences was provided. The complementary structural information provided by FTIR and NMR spectroscopy allows differentiation between the four APP species, as well as the identification of surface-bound species. The important FTIR absorbances and <sup>31</sup>P chemical shifts for each APP species isolated as a solid were identified.

Table IV.II lists selected FTIR absorbances for a 2 wt. % KBr pellet of the solid gamma-aminopropylphosphonic acid as received. The ambient pH of an 18 mM solution of this material was 3.6. FTIR absorbances also were reported

Table IV.I. Acid dissociation constants and  $^{31}\text{P}$  chemical shifts for gamma-aminopropylphosphonic acid species in aqueous solution and isolated in the solid state.

31<sub>P</sub> Chemical Shifts (ppm)

APP SPECIES	Abbrev.	Solutiona	Solid Stateb	pKaa
+NH <sub>3</sub> (CH <sub>2</sub> ) <sub>3</sub> PO <sub>3</sub> H <sub>2</sub>	APP <sup>+</sup>	29.94	33	1.6
+NH3(CH2)3PO3H-	APP	23.85	28	6.8
$^{+}$ NH <sub>3</sub> (CH <sub>2</sub> ) <sub>3</sub> PO <sub>3</sub> <sup>2-</sup>	APP-	20.55	24	11.0
$NH_2(CH_2)_3PO_3^{2-}$	APP <sup>2-</sup>	22.65	26	_

<sup>&</sup>lt;sup>a</sup>These values obtained from reference 12. <sup>b</sup>These values are from this work.

Table IV.II. Selected IR Frequencies (cm<sup>-1</sup>) for solid APP recovered from solution at different pH values.

Hd	Dominant Species	S(H <sub>2</sub> O)	δ(NH <sub>3</sub> )	б(ОН)	v(P=0)	v(PO <sub>3</sub> )	p(NH3)	KH2O) 6(NH3) 8(OH) k(P=O) k(PO3) p(NH3) k(PO3) k(PO3) (CN) k(PO3) k(POH)	v(PO <sub>3</sub> )	v(CN)	v(PO <sub>3</sub> )	v(POH)
		8(NH3)				(PO <sub>3</sub> H <sup>-</sup> )		(PO <sub>3</sub> <sup>2-</sup> )				
HCI	APP+	1644w,	1644w, 1538w 1241m 1157vs 1135vs 1096m	1241m	1157vs	1135vs	1096ш			1007 vs	1007 vs975m 923vs	923vs
2.6	APP	1628w										
ambient APP	APP	1644w,	1644w, 1538w 1242m 1160vs 1137vs 1098m	1242m	1160vs	1137vs	1098m			1008 vs	1008 vs975m 925vs	925vs
3.6		1627w										
NaOH	APP	1646w,	1566w,	1253w,	1164w	1125w	1097m	1646w, 1566w, 1253w, 1164w 1125w 1097m 1069vs 1041vs	1041vs		980m,	935w
7.5	APP-	1627w	1627w 1532w 1236w	1236w							ш696	
NaOH	APP <sup>2</sup> -	1650w	1650w 1583w					1070vs,	1070vs,1053vs		970m	
12								s h				

w = weak; m = medium; vs = very strong; sh = shoulder v, stretching; δ, bending; ρ, rocking

for the solid gamma-aminopropylphosphonic acid recovered from aqueous solution at pH 2.6 in the presence of HCl, and at pH 7.5 and 12 in the presence of identification of APP species in solution at pH values of 2.6 and 7.5 was necessary for the characterization of subsequent reaction products. The identification equilibrium species isolated at pH 12 was included to confirm diagnostic bands. The assignments of absorption bands in Table IV.II parallel those made by Garrigou-Lagrange and Destrade<sup>13</sup> among other workers. 14-17 The bands at 1160  $cm^{-1}$  and 925  $cm^{-1}$  correspond to the V(P=O) and V(POH) stretching frequencies diagnostic of neutral APP species. These bands are present in the spectrum of the solid as received, and in the spectrum of the sample isolated from a solution which had been adjusted to pH 2.6 using HCl. These absorbances were also observed in the spectrum of the solid isolated from a solution which had been adjusted to pH 7.5 using NaOH. The composition of this sample was a mixture of both neutral APP and APP species. As a result, a more complex spectrum was observed for the sample isolated at pH 7.5 than the spectra observed for the samples isolated at pH 3.6 and 2.6, composed chiefly of neutral APP. The APP fraction of the sample formed at pH 7.5 was responsible for the additional very strong absorbances observed at 1070  $cm^{-1}$  and 970  $cm^{-1}$ , symmetric  $V(PO_3)$  vibrations. of diagnostic assignments were confirmed by bands in the spectrum of the

solid isolated from a solution which had been adjusted to pH 12 with NaOH. This sample exhibited absorbances due to the APP<sup>2-</sup> and APP<sup>-</sup> species. Almost all traces of neutral APP disappeared. This was best illustrated by the absence of a strong V(P=0) vibration, typical of highly asymmetric  $PO_3$  groups, in the spectrum. Intense bands diagnostic for symmetric  $V(PO_3)$  groups were observed at 1070 cm<sup>-1</sup> and 970 cm<sup>-1</sup>. A new band, also corresponding to a  $V(PO_3)$  vibration at 1053 cm<sup>-1</sup>, could not be unambiguously assigned to either a symmetric or an asymmetric vibration.

A single anomalous band was included in Table IV.II. The band at 1240 cm<sup>-1</sup> was assigned to a  $\delta$ (OH) vibration. Other workers<sup>15,7</sup> also observed this band. We tentatively assigned the band to a  $\delta$ (OH) vibration here, because the intensity of the band decreases with increasing pH, as indicated in table IV.II.

<sup>1</sup>H decoupled <sup>31</sup>P MAS NMR spectra confirm the identities of the APP species derived from the FTIR results for the four samples isolated at different pH. Table IV.I lists the solution and solid state (this work) <sup>31</sup>P chemical shifts for APP at each level of ionization. The chemical shift values reported for the solution species were determined by Appleton et al.<sup>12</sup> Chemical shifts obtained for the solid samples led to the assignment of 33, 28, and 24 ppm to the APP<sup>+</sup>, APP, and APP<sup>-</sup> species, respectively. The chemical shifts observed for the species isolated as solids were shifted downfield approximately 3 ppm from the

literature solution values. These shifts may arise from stronger hydrogen bonding between  $NH_3^+$  and  $PO_3H^-$  groups because of their close proximity in the crystalline state.

The <sup>1</sup>H decoupled <sup>31</sup>P MAS NMR spectrum of the APP solid as received is shown in Figure IV.1. Two major phosphonic acid environments with chemical shifts of 33 and 28 ppm, and three minor environments having chemical shifts of 5.2, 0.7 and 0.4 ppm probably due to phosphate impurities, were resolved in this spectrum. The intense resonances were assigned to APP<sup>+</sup> and neutral APP, respectively. A <sup>31</sup>P chemical shift of 25.2 ppm has been reported for neutral APP. The hygroscopic nature of the APP solid may give rise to slight variations in chemical shift with hydration. The chemical shift of the APP<sup>2-</sup> species reported in Table IV.I was not determined, but was estimated at 26 ppm from the solution value.

## Reactions of APP with imagolite

Evidence for coupling between APP and imagolite was obtained from <sup>1</sup>H decoupled <sup>31</sup>P MAS NMR spectra of the airdried APP-modified imagolite reaction products. An amount of APP sufficient to provide an equimolar ratio of phosphorus to aluminum was used to form these products. The APP solid was added directly to imagolite suspensions which were immediately adjusted to pH 2.6 (APPIMOGA) and pH 7.5 (APPIMOGB) with HCl and NaOH, respectively. These pH values were chosen to maximize the concentration of a single phosphonic acid species in solution while

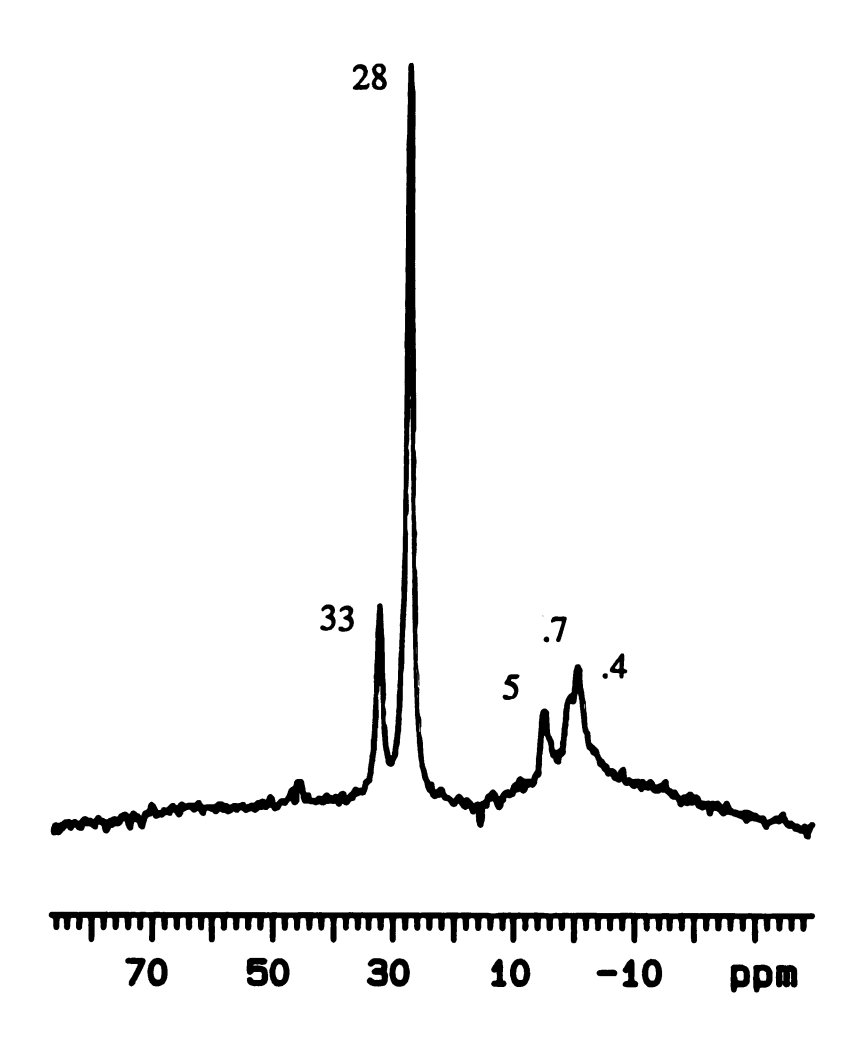


Figure IV.1  $^{1}$ H decoupled  $^{31}$ P MAS NMR spectrum (161.903 MHz) of solid gamma-aminopropylphosphonic acid as received, obtained with a pulse width of 4.8 usec, a relaxation delay time of 60 seconds and a sample spinning rate of 4KHz.

maintaining the structural integrity of the imogolite (and Na-montmorillonite in subsequent reactions). In this way, the products formed from neutral APP and imogolite reactants (APPMONTA) could be compared with those formed between APP and imogolite (APPMONTB). This information may elucidate the role of pH in the formation of the ordered products obtained by reaction of Na-montmorillonite suspensions with APP-modified imogolite suspensions at pH 7.5.

FTIR difference spectra were obtained for the APPmodified imogolite reaction products at each pH. Digital
subtraction of the imogolite FTIR spectrum from the APPmodified imogolite spectra eliminated interference from
strong imogolite SiOAl bands in the APP diagnostic region.
A list of the important vibrations obtained from these
difference spectra is given in Table IV.III. Diagnostic
bands for both symmetric PO<sub>3</sub> and asymmetric PO<sub>3</sub> groups were
observed for APPIMOGA and APPIMOGB samples, suggesting the
presence of multiple APP species in the products.

Two different phosphorus sites were detected in the <sup>31</sup>P MAS NMR spectrum for both of the APP-modified imagolite samples. The phosphorus chemical shifts for the APP treated clay systems are listed in Table IV.IV. Two phosphorus chemical shifts, at 23 ppm and 19 ppm, were observed for the APP-modified imagolite at pH 2.6. The 23 ppm resonance was shifted upfield ≈5 ppm from the chemical shift obtained for the solid APP neutral species

Selected IR Frequencies (cm-1) (KBr pellet) for APP-modified systems. Table IV.III.

Sample,	Dominant Species	S(H <sub>2</sub> O)	K(H <sub>2</sub> O) 6(NH <sub>3</sub> ) 8(OH) v(P=O) v(PO <sub>3</sub> ) p(NH <sub>3</sub> ) v(PO <sub>3</sub> ) v(PO <sub>3</sub> ) v(CN) v(PO <sub>3</sub> ) v(POH)	б(ОН)	v(P=0)	v(PO <sub>3</sub> )	p(NH <sub>3</sub> )	v(PO <sub>3</sub> )	v(PO <sub>3</sub> )	v(CN)	v(PO <sub>3</sub> )	v(POH)
hН		5(NH3)				(PO <sub>3</sub> H <sup>-</sup> )		(PO <sub>3</sub> <sup>2-</sup> )				
APPIMOGA	APP	1694w,	1694w, 1526m 1250w 1148vs	1250w	1148vs			1066vs			988s	926s
2.6 (HCI)		1644w										
APPIMOGB	APP	1660w	1660w 1538m 1248w	1248w		1114vs,		1071vs			8086	918m
7.5 (NaOH)	APP-					s h						
APPMONTA	APP	1646w,	1646w, 1537m 1244m 1155m 1134s	1244m	1155m		1088m,		1043vs,	1043vs, 1010vs,		930vs
5.3		1629w					s h		1022vs s h	s h		
APPMONTB	APP	1660w	1660w 1566w, 1253w	1253w		1130w,		1069vs,	1069vs,1044vs		990w,	930w
7.5 (NaOH)	APP-		1538w			s h		s h			974w	
APPIIM55	APP-	1655w				1121vs,			1055vs			886w,
7.5 (NaOH)						s h						852w

w = weak; m = medium; s = strong; vs = very strong; sh = shoulder v, stretching; 8, bending; p, rocking

Table IV.IV. <sup>1</sup>H decoupled <sup>31</sup>P MAS NMR resonances observed for APP-modified systems.

Samplea	Dominant Species	31P Chemical	Shifts (ppm)	
APPIMOGA pH 2.6	APP	23	19	
APPIMOGB pH 7.5	APP/APP	20	16	
APPMONTA pH 5.3	APP	25		
APPMONTB pH 7.5	APP/APP	23		÷
APPIIM55 pH 7.5	APP <sup>-</sup>	21		3

<sup>&</sup>lt;sup>a</sup> pH was adjusted using aqueous 1M HCl or 1M NaOH solutions.

at 28 ppm, cf. Table IV.I. This chemical shift difference suggests that APP has been coupled to the external surfaces of the imagolite tubes.

The chemical shift of the APP coupled to the external AlOH surfaces of imogolite at pH 2.6 was assigned to the 23 ppm resonance. The resonance at 19 ppm was assigned to neutral APP in close proximity to the internal SiOH surfaces of imogolite. 31P chemical shifts for silicon coupled phosphorus sites are observed downfield from those of aluminum coupled phosphorus sites. Interestingly, the chemical shift of the externally coupled APP occurs near the solution value (cf. Table IV.I) for the neutral APP, the dominant species in solution under the reaction Chemisorption of the negatively charged phosphonate to surface imagolite Al(H2O) + sites, abundant at the reaction pH, may mimic the neutral APP phosphorus environment in solution, resulting in a solution-like chemical shift for the surface-bound APP. The surface immobilization of neutral APP leads to the dissociation of APP+ to reestablish equilibrium. The neutral APP, with a length of ≈6 Å, can diffuse into the 8.7 Å internal imogolite cavity. The intercalation of neutral salts into the imagolite channel has been observed by other workers. 19 Changes in bond lengths and bond angles of the P-O linkages, known to effect drastic changes in chemical shift, 18 may be caused by neutral APP confinement within the hydroxylated channel. In view of these facts, the

19 ppm chemical shift observed for the APP species proposed to occupy the cavity is plausible. The <sup>29</sup>Si MAS NMR spectrum of the APP-modified imagolite products shows a single resonance at -79 ppm due to the uncoupled imagolite silicon sites. This confirms the <sup>31</sup>P NMR result. Covalent bond formation between APP and the SiOH sites located within the imagolite channel would have prompted a more dramatic chemical shift difference between the resonances of the solid APP and the APP-modified imagolite.

The APPIMOGB sample prepared at pH 7.5 exhibited characteristics similar to those of the APP-modified imogolite prepared at pH 2.6. The 31P MAS NMR spectrum contains two phosphorus environments of approximately equivalent intensities, having chemical shifts of 20 and At pH 7.5, the imogolite surface retains a net positive charge, the isoelectric point being pH 9.5. dominant APP species in solution under the reaction conditions were APP and neutral APP. The having a chemical shift of 16 ppm was assigned to the neutral APP intercalated into the imogolite channels in a manner analogous to the APPIMOGA products. Chemisorption of the APP species to the positively charged Al(H2O)+ sites through the phosphate group as observed in the APPMONTA products was still achievable. Charge balance could be maintained by Na cations in solution. The 20 ppm chemical shift was assigned to the APP bound to the external imogolite surface at pH 7.5. This chemical shift

is equivalent to the chemical shift of the APP species in solution (cf. Table IV.I), as observed in the APPIMOGA products. This was again attributed to the effects of APP immobilization on the imagolite surface.

### APP reactions with Na-montmorillonite

The pH dependence of surface coupling between APP and imogolite was coupled with information about APP reactions with Na-montmorillonite. This was a necessary step toward the characterization of the reaction products of Namontmorillonite and gamma-aminopropylphosphonic The addition of a Na-montmorillonite modified imagalite. suspension to an 18 mM APP solution in an amount necessary to achieve 5.9 mole APP/clay equivalent at ambient pH yielded APPMONTA. Similarly, the addition of montmorillonite suspension to an 18 mM solution of APP which had been adjusted to pH 7.5 with NaOH, in an amount necessary to achieve 5.9 mole APP/clay equivalent gave rise to APPMONTB. These products were identified by elemental analysis, FTIR and <sup>1</sup>H decoupled <sup>31</sup>P MAS NMR as intersalate Multiphase reaction products, including unreacted clay phase, were isolated from reactions performed with reduced APP/clay ratios at either pH.

Shown in Figure IV.2A is the powder x-ray diffraction pattern of an oriented film sample of the APPMONTA reaction product. The pH of the solution increased from 3.9 to 5.3 as the reaction proceeded. The 19 Å basal spacing was unchanged after the film was heated at 130°C in air for

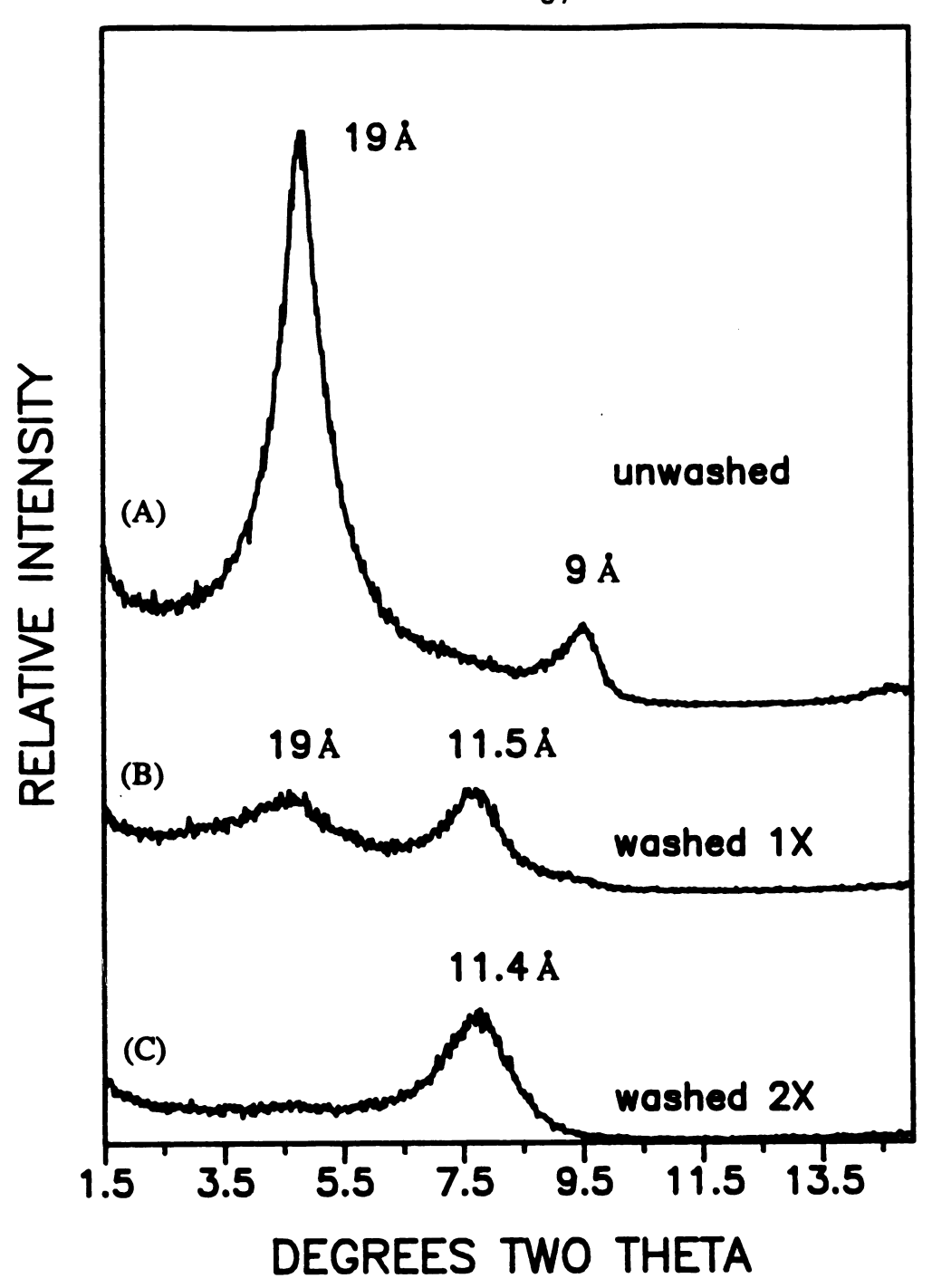


Figure IV.2 X-ray diffraction patterns of (A) APPMONTA, (B) APPMONTA washed once with water and (C) APPMONTA washed twice with water.

36 h. X-ray diffraction patterns of the product after washing with water are shown in Figures IV.2B and IV.2C. The intercalated phosphonic acid was almost entirely removed after the second washing, as indicated by the appearance of a pure clay phase with a basal spacing of 11.4 Å.

The intercalated product formed at pH 7.5 exhibited a basal spacing of 23 Å, appreciably larger than the 19 Å spacing for the product formed at ambient pH. The x-ray diffraction pattern of an oriented film of APPMONTB is shown in Figure IV.3A. The basal spacing was reduced to 21 Å after the film was heated at 130°C in air for 36 h. Washing the 23 Å phase with water resulted in almost complete displacement of this phase by a pure Namontmorillonite phase with a basal spacing of 11.3 Å (cf. Figures IV.3B and IV.3C).

FTIR difference spectra of the 23 Å and the 19 Å reaction products of APP and Na-montmorillonite were obtained by digital subtraction of the Na-montmorillonite FTIR spectrum from the spectra of the APP-modified clay samples. This eliminated interference from the SiOSi and SiOAl clay bands in the region where diagnostic APP bands are observed. Figure IV.4A shows the difference spectra obtained over the frequency range from 4000 to 400 cm<sup>-1</sup>. The absorbances observed in the difference spectra are listed in Table IV.III.

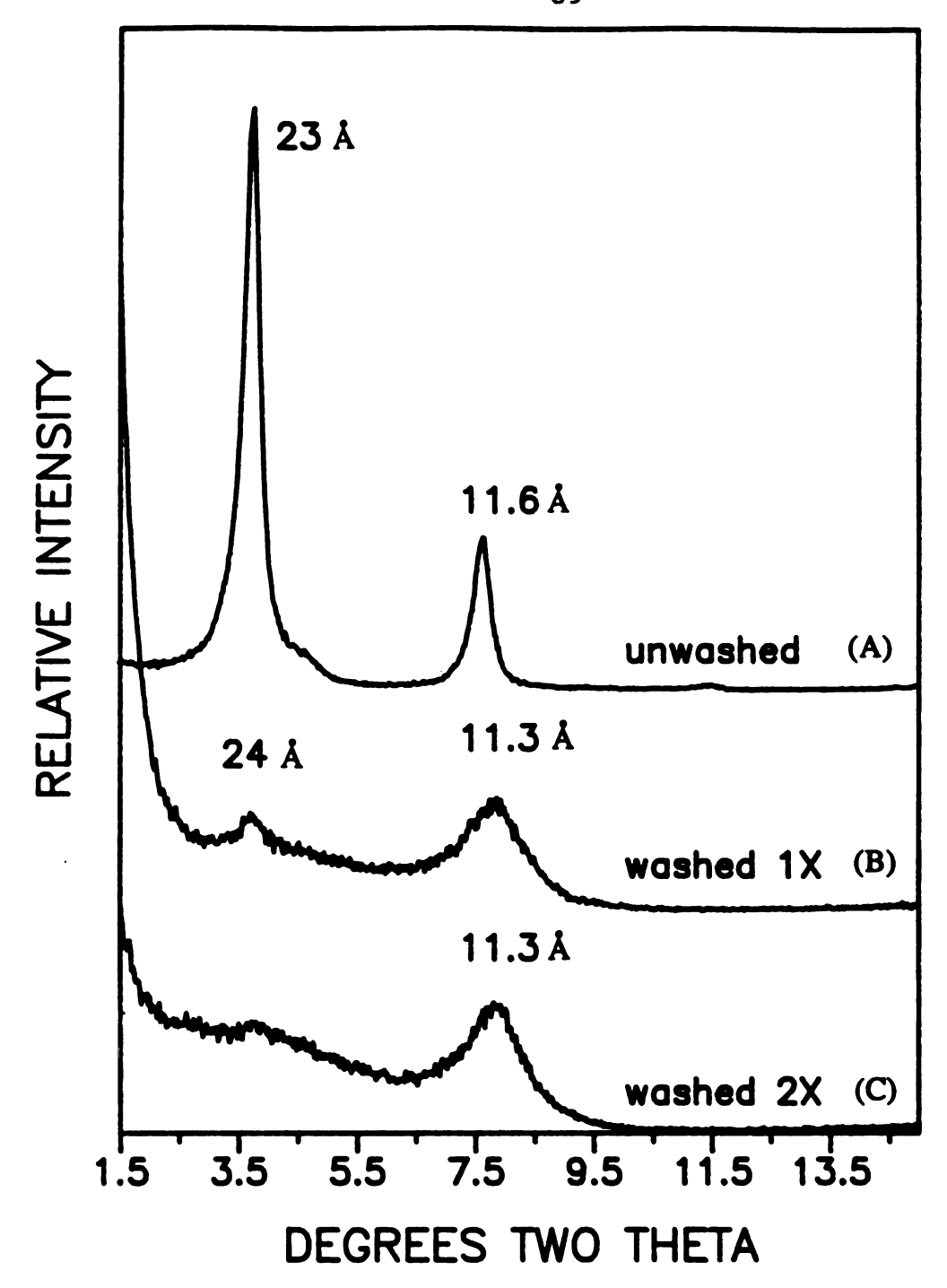


Figure IV.3 X-ray diffraction patterns of (A) APPMONTB, (B) APPMONTB washed once with water and (C) APPMONTB washed twice with water.

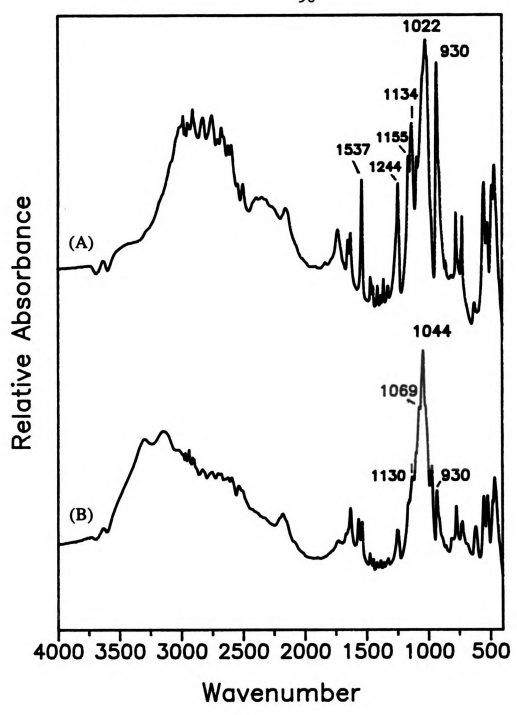


Figure IV.4 FTIR difference spectra (KBr Pellets) of (A) APPMONTA and (B) APPMONTB.

The bands observed in the spectrum of the 19 Å intercalate are analogous to those observed for the neutral APP species (cf. Table IV.II) isolated at ambient pH. The neutral APP species is the dominant species in solution at the reaction pH. Bands diagnostic of asymmetric  $PO_3$  groups located at 1155 cm<sup>-1</sup> and 1134 cm<sup>-1</sup> due to the V(P=0) and  $V(PO_3)$  vibrations, respectively, are observed. A very strong V(POH) band at 930 cm<sup>-1</sup> also indicates the presence of a neutral APP species in the APPMONTA sample.

FTIR evidence for neutral APP is further substantiated by the <sup>1</sup>H decoupled <sup>31</sup>P MAS NMR spectrum of the APPMONTA. One phosphorus resonance was observed with a chemical shift of 25 ppm. Although shifted 3 ppm upfield from the chemical shift assigned to neutral APP in the solid state, cf. Table IV.I, there is sufficient agreement considering possible effects of the close proximity of the clay layers.

<sup>31</sup>P chemical shifts for the APP coupled systems are listed in Table IV.IV. The presence of the neutral APP species within the clay galleries was also supported by the elemental analysis data.

The elemental analysis results for the APP coupled systems are reported in Table IV.V. These results indicate that there are 6.24 APP molecules and 0.88 Na<sup>+</sup> cations per montmorillonite sheet face (Si<sub>8</sub>). A single <sup>31</sup>P NMR resonance indicates that each APP is equivalent. Layer charge balance is maintained in the APPMONTA system by the

Table IV.V. Elemental analysis results for the APP-coupled Na-montmorillonite and APP-coupled imagolite intercalated montmorillonite samples.

SAMPLE	Molecules or atoms per montmorillonite Si <sub>8</sub> unit			
APPMONTA	6.24 APP			
	0.88 Na			
	APP/Na = 7			
APPMONTB	6.00 APP			
	3.92 Na			
	APP/Na = 1.5			
APPIIM55	1.76 APP			
APPIIMOO				
	1.60 Na			
	$\begin{array}{ll} APP/Na &= 1.1 \\ APP/Al^{imogolite} &= 0.028 \end{array}$			
	$APP/Al^{1100yotice} = 0.028$			

Na<sup>+</sup> cations, requiring the intercalated APP units to be electrically neutral.

The bands observed in the FTIR difference spectrum of the 23 Å phase synthesized at pH 7.5 parallel those observed in the spectrum of the pristine APP isolated at pH 7.5, except for the absence of the V(P=0) band. Figure IV.4B shows the FTIR difference spectrum obtained for APPMONTB. Important bands are listed in Table IV.III. FTIR results suggest that both neutral APP and APP species, species dominant in solution under the reaction conditions, are prominent in this sample. The absence of the V(P=0) band, known to be very sensitive to its environment,  $^{20}$  is not unusual.

31<sub>P</sub> NMR spectrum of APPMONTB surprisingly contained only one phosphorus resonance with a 23 ppm chemical shift. A single resonance may have been observed because of proton exchange between the neutral APP and APP that is too rapid to allow differentiation between the two species on an NMR time scale. In this event, the observed chemical shift should be intermediate between resonances of the two exchanging sites, assuming equivalent residence time for the proton at each site. The chemical shift of the neutral APP residing in the gallery was 25 ppm, cf. Table IV.IV. Assuming the effect of the clay layer on APP is similar to that observed for APP, the chemical shift of intercalated APP should be 21 ppm, (shifted 3 ppm upfield from solid APP). The chemical shift expected for fast proton exchange between these two sites is 23 ppm.

The presence of both neutral APP and APP species in APPMONTB is supported by elemental analysis results, cf. Table. IV.V. These results indicate the availability of sufficient Na<sup>+</sup>, after utilizing 0.88 moles to balance the layer charge, to accommodate only 3 moles of APP per Si<sub>8</sub> unit. Since there are 6 moles of APP per Si<sub>8</sub> unit, three moles of APP are required to be electrically neutral.

## APP-modified Imogolite/Na-montmorillonite System

The x-ray diffraction pattern of the product obtained reacting APP-modified imogolite with Naby montmorillonite suspension at pH 7.5 and washing once with water, is shown in Figure IV.5. The products were isolated from reactant ratios of 0.43:1 (w/w) APP:imogolite and (w/w) unmodified imagolite:clay. APP The concentrations, pH and washing procedure were critical to single phase formation. The x-ray diffraction pattern of this product, designated APPIIM55, is characterized by a single reflection at a two theta value corresponding to 55 Å. No reflections were visible in x-ray diffraction patterns of the unwashed material. Pristine APP was found to be x-ray amorphous.

A second reaction was performed at pH 8 on a larger scale. The relative concentrations of the reactants remained the same as in the previous reaction. The x-ray diffraction pattern of the products obtained from this

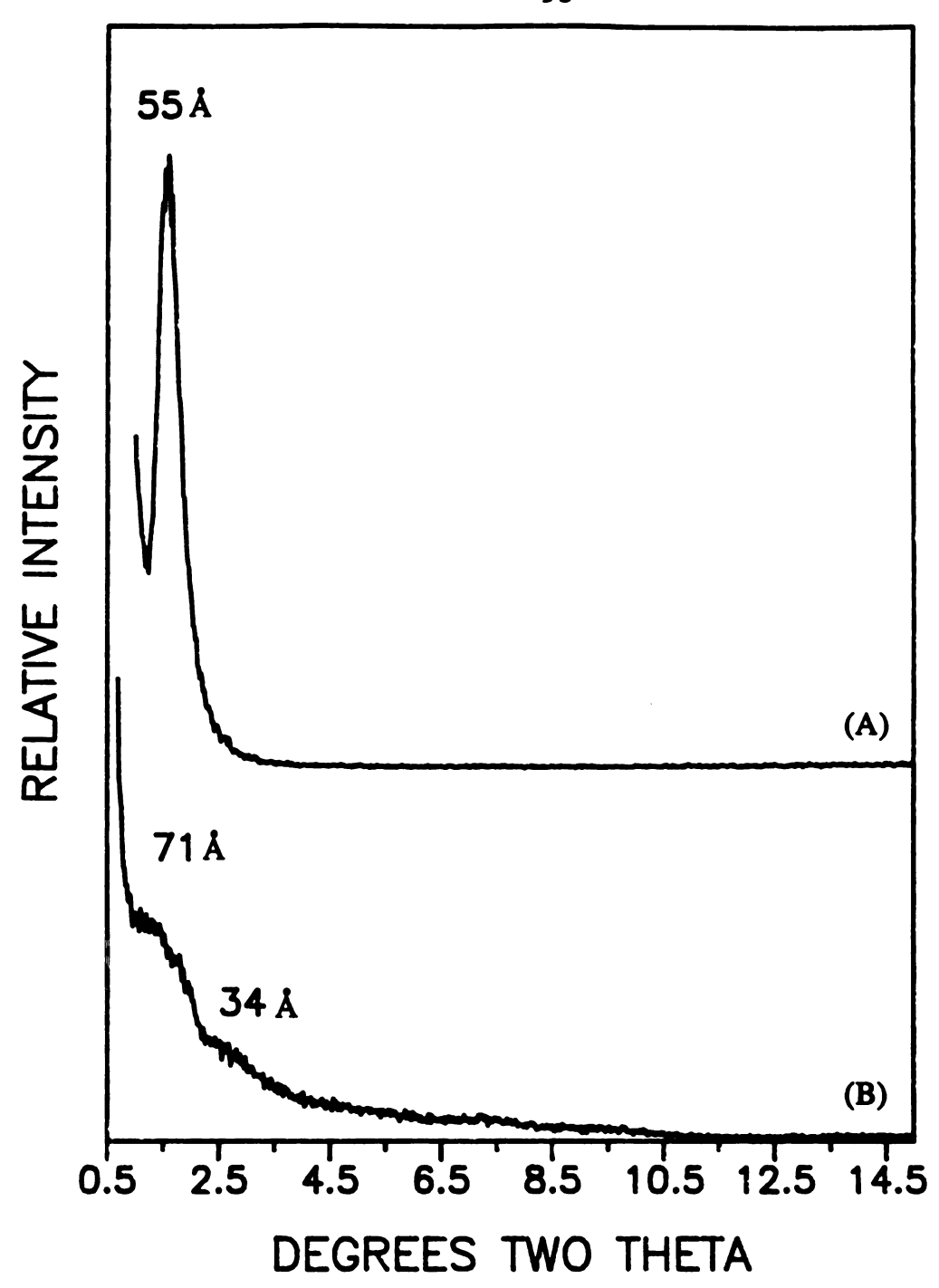


Figure IV.5 X-ray diffraction patterns of (A) APPIIM55 and (B) APPIIM55 after heating at 130°C in air for 48 h.

reaction is shown in Figure IV.6. These products will be referred to as APPIIM75 due to the 75 Å reflection exhibited by the material. A minor second phase was also observed in these reaction products, exhibiting several orders of reflection, having a basal spacing of 36 Å. A 36 Å basal spacing is typical of an unmodified imogolite intercalated montmorillonite (TSLS) phase. This basal spacing corresponds to the sum of the van der Waals dimensions of the clay layer (10 Å) and the hydrated imogolite tubes (≈25 Å). The APPIIM75 material has a composition comparable to that of the APPIIM55 material, but a different distribution of components, as a result of secondary phase formation.

Elemental analysis results from the APPIIM55 sample, listed in Table IV.V, indicate an APP:Na mole ratio of 1.1. This ratio, coupled with the reaction pH, suggests the presence of APP in the complex. The <sup>1</sup>H decoupled <sup>31</sup>P MAS NMR spectrum of APPIIM75 shown in Figure IV.7 supports this conclusion. The spectrum consists of an intense phosphorus resonance with a 21 ppm chemical shift, a intermediate between the 20 ppm resonance observed for the externally bound APP in APPIMOGB and the 23 ppm resonance observed for the fast exchanging APP/APP in APPMONTB, cf. Table IV.IV. A weak resonance was also observed in this spectrum at 3.2 ppm, probably due to the impurities in the starting material. The absence of a 16 ppm resonance in the 31P NMR spectrum of this material indicates that

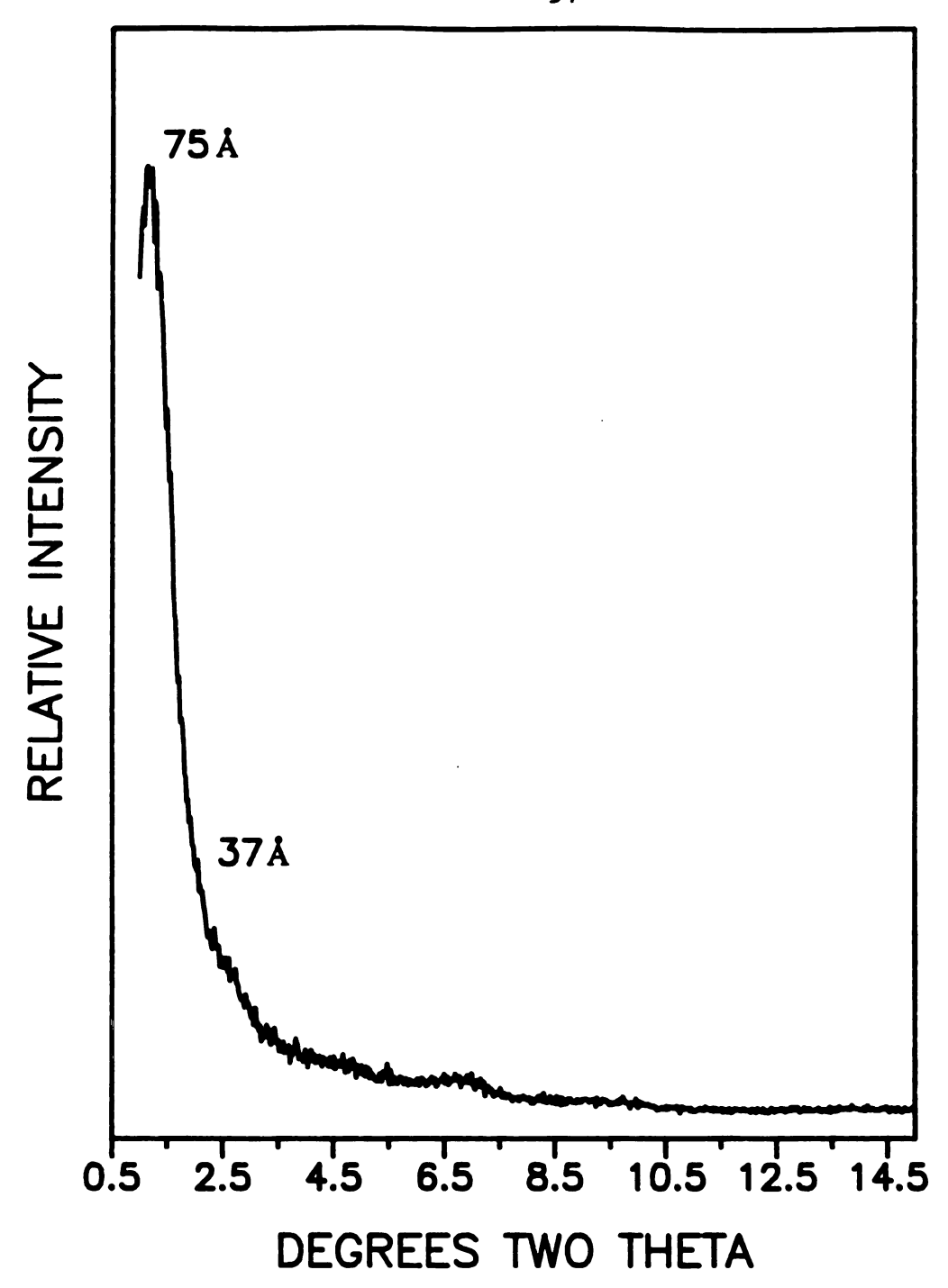


Figure IV.6 X-ray diffraction pattern of APPIIM75.

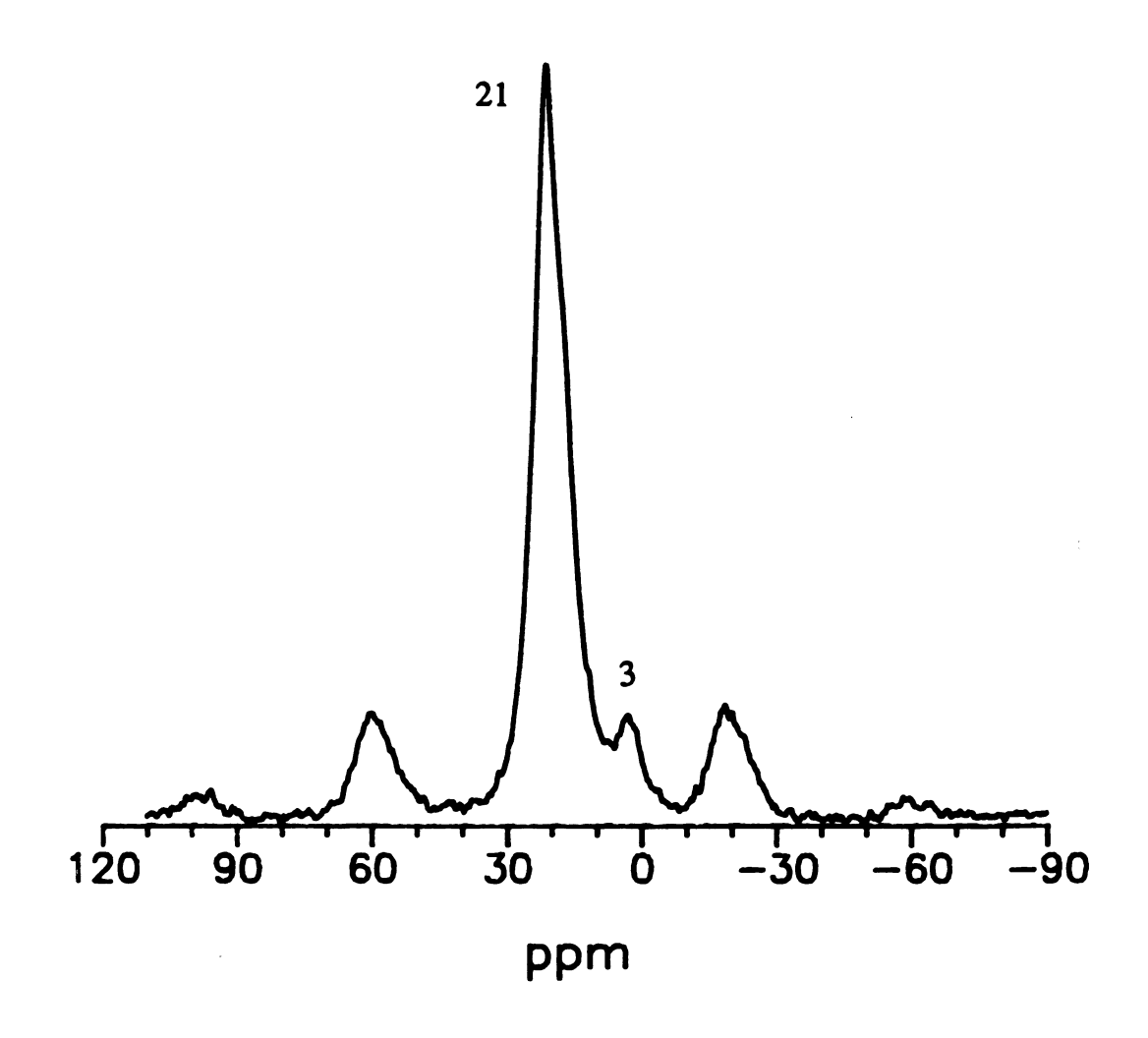


Figure IV.7 <sup>1</sup>H decoupled <sup>31</sup>P MAS NMR spectrum (145.76 MHz) of APPIIM75, obtained with a 3 usec pulse width and a relaxation delay time of 62 sec. (Spectrum courtesy of Kirk Schmitt, Mobil Research and Development Corporation).

washing removes APP from the internal channels of the tubes. FTIR difference spectra obtained for these samples provided no diagnostic bands because of low APP concentrations and the absence of an appropriate reference spectrum.

Additional information on the APPIIM samples was provided by elemental analysis and the <sup>29</sup>Si MAS NMR spectrum for the material. The <sup>29</sup>Si MAS NMR spectrum was obtained for the APPIIM75 sample. Table IV.VI lists the ratio of imogolite silicon (chemical shift -79 ppm)<sup>21,22</sup> to clay silicon (chemical shift -93 ppm). The areas corresponding to each <sup>29</sup>Si resonance were determined from deconvolution analysis of the spectrum. An imogolite to clay ratio of 9:1 (w/w) was calculated from the NMR data, using 12 unit cells per imogolite ring.

The imogolite:clay ratios calculated for the 75 Å products were used to determine that there are 1.76 moles of APP per Si<sub>8</sub> in the APPIIM55 sample. The formation of an APPMONT phase required 6 moles of APP per Si<sub>8</sub>. Therefore, the increase in basal spacing from 36 Å in the TSLS complex to 55 Å in the APPIIM55 sample is not likely to be due to the formation of an imogolite intercalated APPMONTB phase. Similarly, the concentration of APP in the APPIIM55 sample is insufficient to provide for an increased basal spacing due to APPIMOGB intercalated montmorillonite. The APP:imogolite ratio allows for only ten percent of

Table IV.VI. Ratio of the areas obtained by deconvolution analysis of <sup>29</sup>Si NMR resonances at -79 ppm (imogolite) and -93 ppm (Na-montmorillonite), and the corresponding imogolite:clay wt. ratios.

SYSTEM		рН	Si <sup>imog</sup> /Si <sup>clay</sup>	IMOGOLITE/CLAY wt. RATIO
TSLS	1 wash	4	0.67:1	1.5:1
TSLS	1 wash	8	3.53:1	8:1
APPIIM75	1 wash	8	3.93:1	9:1

monolayer coverage where one APP is coupled with each imagolite Al.

Clearly, APP plays an entirely different role in the formation of these materials. Further scrutiny of the <sup>29</sup>Si MAS NMR spectrum allows for correlation of the data for the APPIIM55 system. The 9:1 (w/w) imagolite:clay ratio of the reaction products is larger than the 2.4:1 (w/w) ratio provided by the initial reaction conditions. This means the clay has been preferentially removed in the washing step. A substantial reduction in APP concentration also was observed, as evidenced by the change from .43:1 (w/w) APS:imagolite under the initial reaction conditions to .028:1 (w/w) in the reaction products.

The expansion of the basal spacing beyond 36 Å must be caused by multilayer intercalation of imogolite tubes. APPIIM55 material with a 55 Å basal spacing possesses a 45 Å gallery height. This allows the intercalation of a double layer of imogolite tubes with a 23 Å diameter. The experimentally determined 9:1 (w/w) imagolite:clay ratio, however, is consistent with a material in which a quadruple layer of imogolite tubes arrange themselves between the Correlation of the x-ray diffraction clay layers. patterns, NMR and elemental analyses results is possible only by assignment of the 55 Å reflection to a  $d_{002}$  rather than a  $d_{001}$  reflection. The corresponding 110 Å  $d_{001}$ reflection results in a gallery height of 100 Å. gallery height is consistent with the intercalation of a

quadruple layer of tubes, as predicted by the imogolite to clay ratios.

This description was verified by probing the dehydration behavior of the APPIIM55 material. The x-ray diffraction pattern of APPIIM55 after heating at  $130\,^{\circ}$ C in air for 48 hours, is shown in Figure IV.5B. Heating caused a dramatic decrease in crystallinity and an increase in the  $d_{001}$  reflection to a basal spacing of 70 Å or a 60 Å gallery height. This spacing is consistent with a quadruple layer of tubes which have lost an external layer of water and have been partially collapsed by dehydration.

The characterization of these materials as multiple layers of imogolite tubes between montmorillonite sheets is further supported through nitrogen adsorption data. The surface areas of APPIIM55 and TSLS were measured and found to be equivalent ( $\approx 240 \text{ m}^2/\text{g}$ ). The available surface area for both materials was limited to the internal channels of the tubes and the spaces between tubes arising from their close packing between the clay layers. Therefore, surface area should be independent of the number of rows of tubes stacked between the clay layer.

Confirmation of the intercalation of close-packed imogolite multilayers was also obtained by calcination experiments. The APPIIM55 material should retain an appreciable surface area after it has been calcined at 350°C due to stabilization of the intercalated tubes toward dehydroxylation. Imogolite which has not been

intercalated, however, undergoes dehydroxylation at this temperature, resulting in a reduction in surface area following calcination.

A poorly ordered material with an imagolite:clay ratio of 8:1 (w/w) was formed under reaction conditions in absence of APP, but otherwise identical to those used to synthesize APPIIM75. This material, like APPIIM55, had an imogolite composition in excess of that required to obtain a monolayer of intercalated tubes. Unlike APPIIM55, this material exhibited weak x-ray diffraction reflections typical of the TSLS complex. The poorly ordered reaction products obtained in absence of APP, were composed of TSLS and disordered imagolite phases. The surface area of this material was equivalent to that obtained for highly ordered TSLS complexes. The effect of calcination on the APPIIM55 material was compared with the effect of calcination on the disordered TSLS material. The surface area of APPIIM55 after calcination at 350°C was 192 m<sup>2</sup>/g. The surface area of the disordered TSLS material after calcination at 350°C was only 105  $m^2/q$ .

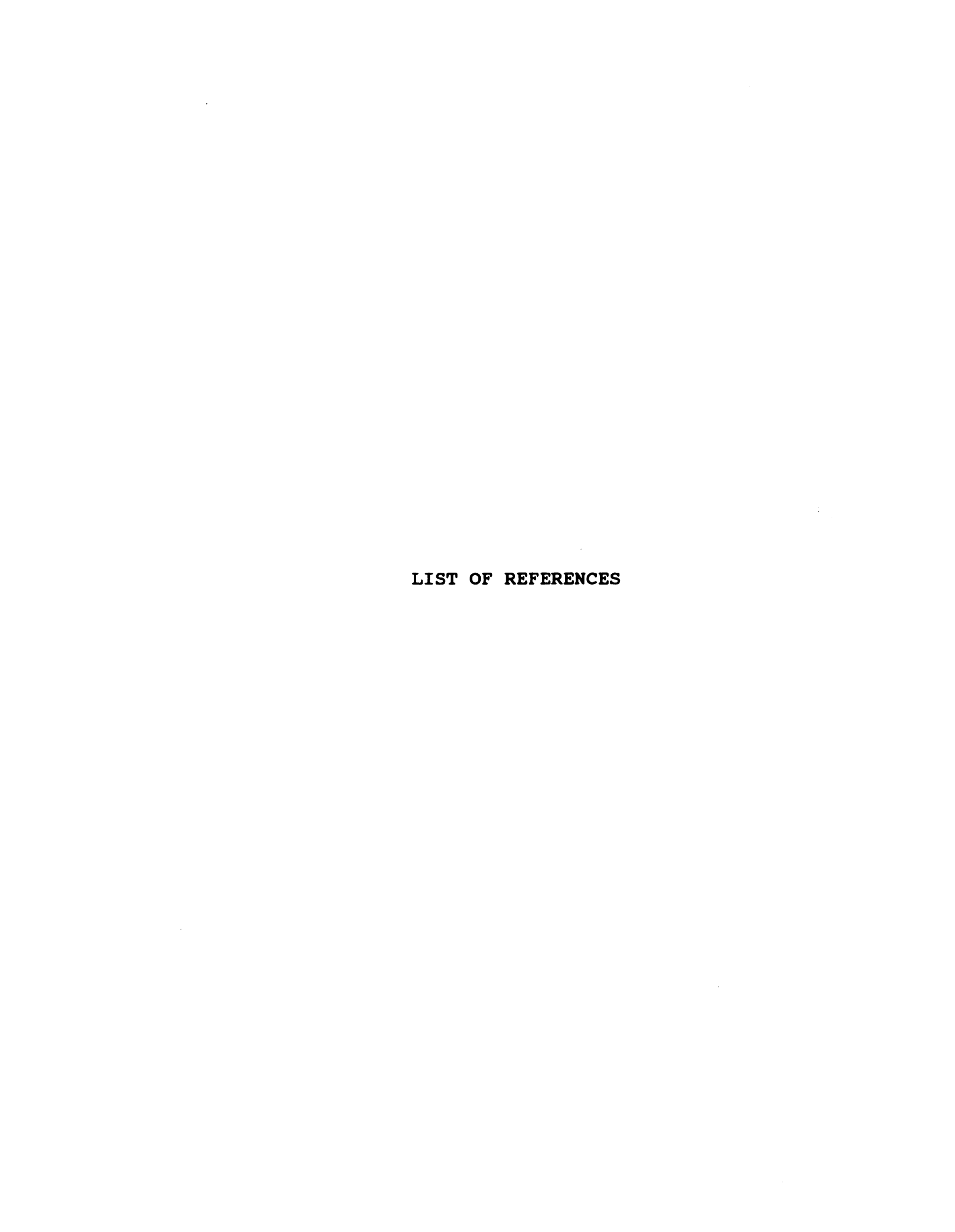
## D. CONCLUSIONS

Highly ordered products were obtained from reactions between APP-modified imogolite and Na-montmorillonite. Specific reactant concentrations, pH and washing procedures were critical to single phase formation. These reaction products were characterized by <sup>29</sup>Si and <sup>31</sup>P MAS NMR, FTIR,

x-ray diffraction, elemental analysis and nitrogen adsorption measurements. These results provided a description of the material as quadruple layers of close-packed imogolite tubes intercalated between the layers of Na-montmorillonite. The role of APP in the reaction appears to involve ordering small bundles of imogolite tubes in solution. Selective removal of Na-montmorillonite from the reaction with washing occurs both in the presence and in the absence of APP.

The reaction of APP with Na-montmorillonite results in the formation of an intersalate complex. At an ambient reaction pH of 5.3, the neutral APP is the species which occupies the gallery. At pH 7.5, in the presence of NaOH, APP and APP species, found to undergo rapid proton exchange, occupied the gallery.

APP was found to chemisorb to the  $Al(H_2O)^+$  sites on the external imogolite surface. Dialysis of APP-coupled imogolite samples against deionized water promoted desorption of APP from the surface. APP was also found to simultaneously intercalate into the channels of the imogolite tubes.



## LIST OF REFERENCES

- 1. Cradwick, P.D.G.; Farmer, V.C.; Russell, J.D.; Masson, C.R.; Wada, K.; Yoshinaga, N. Nature Phys. Sci. 1972, 240, 187.
- 2. Johnson, I.D.; Werpy, T.A.; Pinnavaia, T.J. J. Am. Chem. Soc. 1988, 110, 8545.
- 3. Werpy, T.A.; Michot, L.J.; Pinnavaia, T.J. In Novel Materials in Heterogeneous Catalysis; Baker, R.T.K.; Murrell, L.L., Eds.; American Chemical Society: Washington, D.C., 1990.
- 4. Plueddemann, E.P. Silane Coupling Agents; Plenum: New York, 1982.
- 5. Johnson, L.M.; Pinnavaia, T.J. Langmuir 1990, 6, 307.
- 6. Davis, G.D.; Ahearn, J.S.; Venables, J.D. J. Vac. Sci. Technol. 1984, A2, 763.
- 7. White, H.W.; Crowder, C.D.; Alldredge, G.P. J. Electrochem. Soc. 1985, 132, 773.
- 8. Templeton, M.K.; Weinberg, W.H. J. Am. Chem. Soc. 1985, 107, 774.
- 9. Ramsier, R.D.; Henriksen, P.N.; Gent, A.N. Surf. Sci. 1988, 203, 72.
- 10. Farmer, V.C.; Fraser, A.R. Dev. Sedimentol. 1978, 27, 547.
- 11. Glowiak, T.; Sawka-Dobrowolska, W. Acta. Cryst. 1980, B36, 961.
- Appleton, T.G.; Hall, J.R.; Harris, A.D.; Kimlin,
   H.A.; McMahan, I.J. Aust. J. Chem. 1984, 37, 1833.
- 13. Garrigou-Lagrange, C.; Destrade, C. J. Chim. Phys. 1970, 67, 1646.
- 14. Destrade, C.; Garrigou-Lagrange, C. J. Chim. Phys. 1970. 67, 2013.
- 15. Menke, A.G.; Walmsley, F. Inorg. Chim. Acta 1976, 17, 193.

- 16. Fenot, P.; Darriet, J.; Garrigou-Lagrange, C.; Cassaigne, A. J. Mol. Struct. 1978, 43, 49.
- 17. Sahni, S.K.; van Bennekom, R.; Reedijk, J. Polyhedron 1985, 4, 1643.
- 18. Harris, R.K.; Merwin, L.H.; Hagele, G. Mag. Res. Chem. 1989, 27, 470.
- 19. Clark, C.J.; McBride, M.B. Clays Clay Miner. 1984, 32, 300.
- 20. Thomas, L.C. Interpretation of the Infrared Spectra of Organophosphorus Compounds; Heyden: London, 1974.
- 21. Barron, P.F.; Wilson, M.A.; Campbell, A.S.; Frost, R.L. Nature 1982, 299, 616.
- 22. Goodman, B.A.; Russell, J.D.; Montez, B.; Oldfield, E.; Kirkpatrick, R. J. Phys. Chem. Miner. 1985, 12, 342.

